AFOSR SCIENTIFIC REPORT
AF-AFOSR 959-65

DEFLAGRATION AND DEFLAGRATION LIMITS OF SINGLE CRYSTALS OF AMMONIUM PERCHLORATE

BY

D. M. WATT, JR. AND E. E. PETERSEN

FINAL REPORT

GRANT NO. AF-AFOSR 959-65
FOR THE PERIOD JUNE 1, 1965 TO JUNE 30, 1968

PRINCIPAL INVESTIGATOR: E. E. PETERSEN

PREPARED FOR
THE AIR FORCE OFFICE OF SCIENTIFIC RESEARCH
OF THE OFFICE OF AEROSPACE RESEARCH
UNDER CONTRACT NO. AF-AFOSR 959-65

AFOSR SCIENTIFIC REPORT
AF-AFOSR 959-65

DEFLAGRATION AND DEFLAGRATION LIMITS OF SINGLE CRYSTALS OF AMMONIUM PERCHLORATE

BY

D. M. WATT, JR. AND E. E. PETERSEN

FINAL REPORT

GRANT NO. AF-AFOSR 959-65
FOR THE PERIOD JUNE 1, 1965 TO JUNE 30, 1968

PRINCIPAL INVESTIGATOR: E. E. PETERSEN

PREPARED FOR
THE AIR FORCE OFFICE OF SCIENTIFIC RESEARCH
OF THE OFFICE OF AEROSPACE RESEARCH
UNDER CONTRACT NO. AF-AFOSR 959-65

ABSTRACT

The research reported here consisted of the experimental determination of the deflagration pressure limit and the deflagration rate for single crystals of ammonium perchlorate over an extended range of ambient temperatures and pressures and some preliminary results on the effects on ignition and deflagration of doping ammonium perchlorate (AP) with potassium permanganate.

Using a new technique, the deflagration pressure limit was measured by imposing a known linear temperature gradient along the length of the AP sample and igniting the warmer end. The pressure was adjusted so that the flame would not propagate through the entire solid, and the length remaining unburned determined the limiting solid temperature corresponding to the set pressure. For both AP single crystals and pressed pellets the limiting pressure fell essentially linearly from 385 psia to 225 psia over the solid temperature range of -40 to 50°C, and from 50 to 80°C the slope of the limiting pressure versus the solid temperature decreased considerably. No difference was observed when using helium in place of nitrogen as the ambient atmosphere.

The AP single crystal deflagration rates were measured using high-speed motion photography and were essentially the same in helium and nitrogen ambient atmospheres. As the pressure was increased the burning rate increased, went through a maximum and a minimum, and then continued to increase. The

burning rates increased monotonically with increasing ambient temperature.

Comparison of burning rates of large single crystals prepared in this laboratory with those prepared in another laboratory indicated the possibility that catalytically active impurities were present in the single crystals grown from AP from different sources even though the impurity concentration was extremely low.

In direct contrast to the catalytic effect of $KMnO_4$ on AP thermal decomposition, a preliminary study showed that 0.4-2.0 mole % $KMnO_4$ isomorphously substituted into the AP crystal lattice prevented deflagration from occurring.

TABLE OF CONTENTS

TABLE OF CONTENTS continued

LIST OF TABLES

LIST OF FIGURES

LIST OF FIGURES continued

CHAPTER I

INTRODUCTION

Ammonium perchlorate, NH_4ClO_4, is one of the most commonly used oxidizers in composite solid propellants and has been the subject of intensive research for a number of years. In the propellant formulation granulated ammonium perchlorate (AP) is generally mixed with fuel, catalyst, and plasticizer or binder to form the composite propellant grain. A considerable amount of research has been concerned with propellant formulations; however, the heterogeneity of the composite propellant makes the description of the ignition and deflagration processes very complex and emphasizes the need for a better understanding of the fundamental mechanisms of solid propellant ignition and deflagration. Since the reactions of AP alone strongly influence both the ignition and burning of composite propellants, this research program has been focused on the ignition and deflagration of pure AP in continuation of the work of V. S. Engleman (10).

The ignition and the deflagration of solid propellants have been studied generally as separate and distinct problems, but clearly the two studies are not independent and viewing the two problems together may add considerable insight into the basic processes involved. For example, a theory for ignition should predict the steady state deflagration rate as time approaches infinity, and a model for steady state deflagration should indicate the necessity for an

ignition process before the propellant will deflagrate. (These examples will be discussed in detail later.) Viewing AP research as a single problem makes a complete critical review of the literature impractical, if not undesirable, and accordingly an effort will be made here to give some perspective on the research that has gone into the present understanding of the physicochemical processes involved in the ignition and deflagration of AP. References to review articles on various aspects of the overall problem are listed for supplementary reading.

No experimental techniques have been developed to determine the complete sequence of reactions leading from solid AP to the final reaction products during the ignition transient and at steady state. Problems encountered in such a study include the transient nature of the ignition process during which the length of the gas-phase reaction zone decreases to less than 100μ at steady state deflagration (16) and the receding solid surface which may be quite irregular with a considerable amount of subsurface reaction. The use of sampling probes in the reaction zone to follow the course of the reaction is, therefore, impractical; accordingly, models are necessary to utilize direct experimental measurements. Friedman's review (16) of experimental techniques in solid combustion research shows that no experimental data have been taken which characterize the fundamental processes involved in either AP ignition or deflagration, and, hence there are no data from which unambiguous reaction rate

parameters can be derived for these processes. Consequently the interpretation of most data on AP ignition and deflagration is dependent upon assumed theoretical models of the overall processes; by fitting the data to these models deductions can be made only about the various reactions which have been assumed to comprise the overall processes. This problem is made more serious by the fact that the large number of fitted parameters in the ignition and deflagration models make it extremely difficult to distinguish experimentally between the various possible theories. Since there is no consensus on the correctness of the different theories, there is a need for more complete theories which take into account all the relevant data on ignition and deflagration and a need for well designed experiments to test the theories more rigorously.

Consider now some of the various theoretical models which have been used to link the experimental data with the fundamental processes involved in AP ignition and deflagration. The literature is extensive and for more details one should refer to more complete reviews of individual topics (10,13,14,30,35,38,44). Solid propellant ignition is generally characterized by measuring the ignition delay as a function of the applied ignition heat flux. Since it is difficult to define experimentally the exact ignition point, the ignition delay is usually measured as the time between the application of the ignition stimulus and the first detectable light from the flame. The experimental ignition

delay is correlated with the fundamental processes by assuming that one process predominates during ignition; i.e., when this processes reaches runaway conditions, ignition has occurred. The controlling step has been postulated to be the solid-phase reaction (22), the gas-phase reaction (21), and a heterogeneous, gas-solid reaction (2). Price et al. (38) have presented a thorough review of these theories and the experimental results indicate that different theories may apply to different propellants. It is extremely difficult to distinguish clearly among these models with only ignition delay data. Virtually all these ignition models apply only up to runaway conditions and are incapable of predicting stable deflagration conditions. In addition, AP and AP composite propellants will not deflagrate in an inert atmosphere below a limiting pressure, and a useful ignition theory should indicate a similar behavior. Although it seems possible that the reaction mechanism changes throughout the ignition transient, extension of ignition theories to include deflagration conditions would significantly increase the data applicable for testing the theories. Since it appears to be quite difficult to determine experimentally the reactions occurring during ignition, it seems logical to try to extend the theories to include as much of the existing data as possible.

The most generally measured property of solid propellant deflagration is the rate of surface recession [see Pittman's review of this data (35)], and a theoretical model

of the burning is necessary to correlate this overall measurement with the kinetic processes occurring in the gaseous and condensed phases. By assuming that solid deflagration occurs in two steps, the reaction of the solid to form gaseous intermediates and the gas-phase reaction to form the final products, and by applying adiabatic laminar flame theory to the gas-phase reaction, relatively simple models of solid deflagration have been formulated. Spalding (50) reviewed the literature leading up to the formulation of this model, and Johnson and Nachbar (29) made a thorough mathematical analysis of this model. Friedman and Levy (14) presented a slight variation of this basic formulation along with a review of the application of the theory to AP and AP composite propellants. Unfortunately, these theoretical formulations apply only to burning rate data and do not explain two of the most significant characteristics of solid propellants: the deflagration pressure limit, which is about 20 atm for ammonium perchlorate (23,32), and the necessity for an ignition process before deflagration will occur. At ordinary ambient temperatures AP and AP composite propellants are generally quite stable and must be ignited to deflagrate. In addition, a complete analysis of the steady-state conditions for AP should admit the essentially non-reactive stable steady state as well as the deflagration stable steady state. As with models applied to solid propellant ignition, it appears that a more complete theoretical analysis of deflagration would permit more data, such as

the pressure limit data and the fact that AP must be ignited, to be used in testing the theory.

Another important aspect of AP deflagration is the non-equilibrium nature of the combustion products as revealed by product temperature analysis (15) and product gas analysis (32). The adiabatic flame temperature is about 1400°K while the measured flame temperature is about 1200°K. An analysis of the collected products indicated considerably more NO than would be present at equilibrium and the product distribution changed with pressure. Thermo-chemical calculations showed the non-equilibrium product distribution to be generally consistent with the low flame temperature. Although these measurements are extremely important for understanding the overall process, they do not reveal the details of the many intermediate physicochemical processes.

The size of the flame zone increases with decreasing pressure, but even near the deflagration pressure limit the flame zone is too small to probe experimentally. Reactions comparable to deflagration may be induced at one atmosphere pressure by adding a heat flux to the reacting surface. By doing this, Friedman and von Elbe (12) have shown that the thickness of the flame zone can be increased to where the intermediate reactions can be studied experimentally. This procedure shows promise of adding considerably to the understanding of solid deflagration, but it will have to be shown that the same reactions occur at the low pressure with the added heat flux as occur under normal deflagration conditions.

Similarly there have been extensive efforts to isolate the reactions occurring in the solid phase during deflagration by studying the thermal decomposition of AP. This research has been reviewed quite thoroughly by Pittman (35) and Keenan (30). The applicability of thermal decomposition rate data taken in the range of 200 to 300°C depends upon the assumption that these data can be extrapolated to deflagration conditions where the surface temperature is on the order of 600°C. The surface temperature has been measured by several techniques (3,36,37,42), but experimental complications have prevented a precise measurement of this temperature. If an activated process is involved at the surface, a relatively small change in surface temperature could account for a large change in the rate of surface recession. In addition, it is quite difficult to determine exactly what temperature is measured because the surface is quite irregular on the microscopic scale and is apparently covered with a frothy, molten layer (7). When AP is heated slowly it decomposes and sublimes (27) rather than melting; hence it is difficult to determine the physical and chemical properties of the observed molten layer at the deflagrating surface. Observation of surface reactions is further complicated by the transformation of AP from the orthorhombic crystal structure to the cubic structure at 240°C: this endothermic process requires about 8 kcal/mole (27). Even with all of this experimental effort the understanding of the solid-phase reactions occurring during deflagration is still

quite incomplete and a simplified view of these reactions is necessary in the formulation of a complete theoretical model of deflagration.

From the foregoing introduction it is clear that no single study can expect to answer all the remaining questions. Since stable steady-state deflagration cannot be understood as an extension of present theories of AP ignition and since the necessity of an ignition process is not explained by current theories of AP deflagration, this research presents a unified theoretical approach to ignition and deflagration in an effort to unite these separate theoretical efforts and to emphasize that ignition and deflagration, by their nature, must not only be compatible, but must necessarily be linked together. Because of the approximations necessary to formulate a model which could be treated analytically, this theory remains qualitative and must await a more rigorous formulation and solution before it can be fitted to the data. For this reason the experimental results of this research are presented first, and the experimental program was designed to obtain the different types of data over extended ranges of conditions which will be useful when a quantitative, unified theory of ignition and deflagration becomes available.

A qualitative steady-state analysis of AP deflagration has provided the necessary organization and basic direction for this research program. Using a one-dimensional model for solid deflagration, one may make a stability

analysis by considering the heat balance across any plane perpendicular to the burning direction. If the net heat flux into this plane is zero, then the reactions are at steady state. If, after a small perturbation from this steady state, the system returns to this steady state then it is a stable steady state, but, if the small perturbation causes the system to reach another steady state or no steady state, then it is an unstable steady state. Deflagration is a stable steady state, but an unstable steady state is generally involved in any ignition process. In addition, at non-steady state conditions the value of the net heat flux into the chosen plane is important in determining the rate of approach to steady state either during ignition or after a disturbance in the system. Consequently a better understanding of this heat balance could help to explain both ignition and deflagration.

Specifically, consider the heat balance across the plane dividing the flame and surface reactions from the AP which is being heated from the ambient temperature T_a to the surface temperature T(0). For pure AP in an inert environment the heat flux Q_F from the flame and surface reactions across this plane could be expected to be a function of the pressure and surface temperature; i.e., $Q_F = Q_F[P, T(0)]$. Since gas-phase reactions are involved, Q_F would be expected to increase with pressure. A qualitative representation of Q_F as a function of T(0) is given in Fig. I-1. The initial exponential rise of Q_F with T(0) is characteristic of

——— Q_F, heat flux into the solid from gas phase and surface reactions.

----- Q_B, heat flux to heat solid from the ambient temperature T_A to T(0).

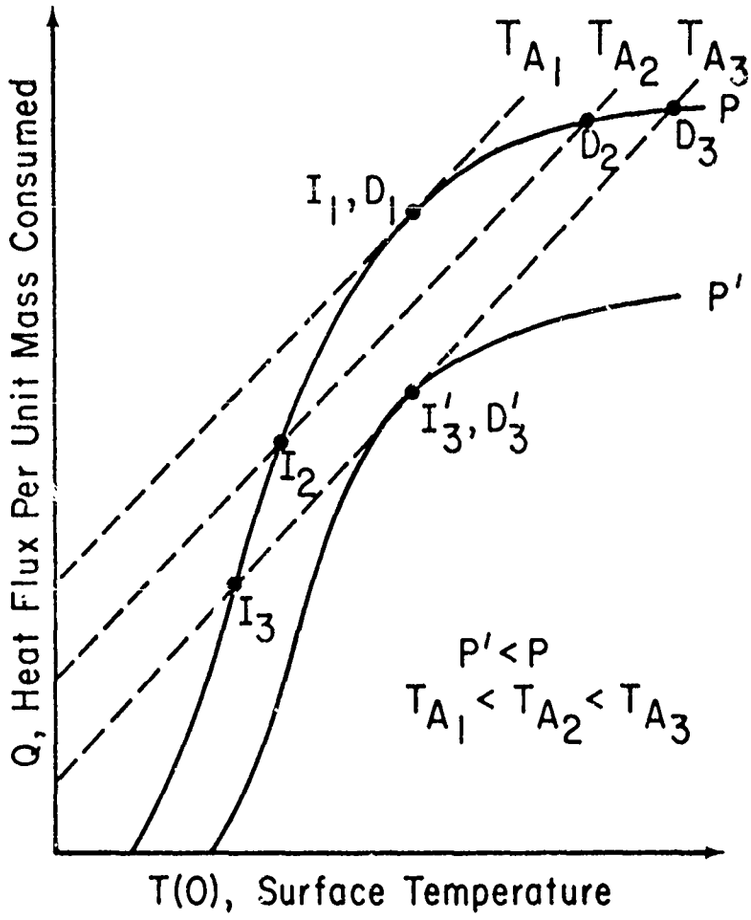

Fig. I-1. Determination of $Q_F = Q_B$ for steady state combustion.

chemical reactions with Arrhenius-type temperature dependence; the leveling off of Q_F is caused by heat and mass transport limitations which lead to a depletion of reactants. This leveling off of Q_F as T(0) becomes large is indicated by standard solid combustion theories with the thermal diffusivity approximately equal to the mass diffusivity (the Lewis number approximately equal to unity); if this did not occur, Q_F would rise exponentially and explosive conditions would be indicated. In analogous fashion, Q_B, the heat flux required to heat the solid from T_a to T(0), would be expected to be a function only of the ambient temperature T_a and the surface temperature T(0); $Q_B = Q_B[T_a, T(0)]$. Since there are no chemical reactions involved in Q_B, it is well approximated by a straight line in Fig. I-1.

The net heat flux into this plane is zero when $Q_F = Q_B$; i.e., steady state conditions are indicated by intersections of Q_F and Q_B in Fig. I-1. As in the stability analysis of a perfectly stirred tank reactor one, two, or three steady states are possible in different regions of operation; consequently regions of pressure and ambient temperature can be designated by the number of possible steady-state conditions occurring at any pressure and temperature within the region. Considering ambient temperature T_{a_2} and pressure P in Fig. I-1 the two Q_F--Q_B intersections indicate two reactive steady-state solutions, and the nonreactive steady state, in which AP is so commonly encountered, could be considered a third intersection below the

scale of Fig. I-1. The non-reactive steady state is stable since a significant ignition stimulus is required to ignite the AP, a process which involves a change from the non-reactive condition to the stable steady-state deflagration at the intersection labeled D_2. In addition, if the igniter is removed too quickly, the reactions decay immediately, and, if the igniter is too weak, the AP will decompose as long as the igniter is on, but it will not ignite and deflagrate. These observations point to the existence of an unstable steady state or ignition point labeled I_2; a small perturbation from this steady state causes either quenching or ignition to point D_2. The ignition stimulus is required to raise the surface temperature beyond this ignition point to obtain deflagration. At a given ambient temperature, for instance, T_{a_3} in Fig. I-1, these three steady states occur at any pressure above P′; likewise at a set pressure P three steady states occur at ambient temperatures above T_{a_1}. Consequently these reactive steady states should be determined over a wide range of both temperature and pressure. The burning rate of the solid is generally used to characterize the deflagration steady state, and Chapter III describes the measurement of the burning rate of ammonium perchlorate for pressures ranging from the minimum pressure which will support deflagration to 5000 psia and for ambient temperatures ranging from -30 to 90°C. Since the ignition point is an unstable steady state it cannot be maintained in practice throughout this range of pressures and temperatures and

could not be measured.

As the pressure is reduced toward the pressure limit or as the ambient temperature is reduced towards the limiting temperature corresponding to the set pressure the ignition point I and the deflagration condition D move closer until at the limiting condition the two points coincide exactly as shown in Fig. I-1 at point I_1, D_1 and at point I_3', D_3'. At this deflagration pressure limit only two steady states are possible: the non-reactive steady state and the reactive Q_F--Q_B point of tangency where the stable deflagration steady state and the unstable ignition steady state coincide. Thus the deflagration pressure limit, which is a unique function of the ambient temperature, defines the line or boundary between the region of pressures and temperatures with three possible steady states and the region with the single non-reactive steady state. Since experimental characterization of the unstable steady state is impractical in general because of the transient nature of the ignition process, the measurement of this unique limiting condition where the ignition point coincides with the deflagration condition is of considerable fundamental importance. In Chapter II a new technique is described which was used to determine the AP deflagration pressure limit for ambient temperatures ranging from -40 to 80°C.

The region below the pressure limit was not investigated in this program since there are no reactive steady state conditions. However, in this range of pressures and

temperatures a heat flux can be applied to an AP surface to make up the difference between Q_F and Q_B to produce a pseudo-steady state reaction at a rate comparable to deflagration, but, when this heat flux is removed, these reactions quickly decay to zero (12).

Catalysts strongly influence the deflagration pressure limit, the burning rate and the ignition delay time, but the role of the catalyst in the fundamental processes of the overall reaction is not clear. Most studies have been concerned with pellets pressed from mechanical mixtures of catalyst and AP, but the growth of large single crystals of AP doped with catalyst permits the study of a homogeneous solid catalyst. Chapter IV describes a preliminary investigation of the catalytic effects of potassium permanganate isomorphously substituted into the AP crystal lattice.

Thus the experimental program is presented in Chapters II, III, and IV. In Chapter II the measurement of the boundary of the region of pressures and ambient temperatures in which AP will deflagrate is reported. Then in Chapter III this deflagration region, characterized by measurements of AP single crystal burning rates over an extended range of pressures and ambient temperatures, is discussed. In Chapter IV the results of a preliminary investigation of the catalytic effects of $KMnO_4$ on AP deflagration are presented. These data can be understood in a qualitative sense from the theoretical approach presented in Chapter V, but a quantitative formulation of this theory

will be necessary before the data can actually be fitted to the theoretical model.

CHAPTER II

THE RELATIONSHIP BETWEEN THE LIMITING PRESSURE AND THE SOLID TEMPERATURE FOR THE DEFLAGRATION OF AMMONIUM PERCHLORATE

Introduction

Although it has been clearly demonstrated that there is a limiting pressure below which pure ammonium perchlorate (AP) will not deflagrate in an inert atmosphere, relatively little experimental attention has been paid to the systematic measurement of this limit and no satisfactory theoretical explanation presently exists. The discussion in Chapter I indicated that at the deflagration pressure limit the unstable steady state, or ignition point, and the stable deflagration steady state coincide exactly. This is the only condition where this unstable steady state can be determined in a straightforward manner, and data on this limiting condition will be extremely useful in the evaluation of theoretical models of deflagration. Furthermore, it has been shown (54) that the pressure below which AP cannot be ignited can be limited by the strength of the ignition source, but for sufficiently strong igniters, the ignition pressure limit and the deflagration pressure limit should be identical. Hence theories for the ignition and for the steady deflagration of AP must ultimately agree at this limiting condition. Consequently the present experimental work was undertaken to determine the limiting pressure more precisely

by using a new experimental technique.

The deflagration pressure limit has been conventionally determined as the pressure below which a flame will not propagate through the solid. For example, an AP crystal is ignited and entirely consumed at pressure P_1, but at pressure $P_1 - \Delta P$ the deflagration wave will not propagate when the ignition stimulus is removed. An experimental value of a limiting pressure range is thus found which depends upon how small ΔP can be made with reproducible results. This procedure for measuring the pressure limit is, at best, difficult and subject to wide variations in results caused by differences in the strength of the ignition source and by the transient nature of the ignition process. Using this technique Friedman, Nugent, Rumbel, and Scurlock (15) reported that the pressure limit was a strong function of the particle size of the AP powder which was pressed into pellets for burning and of the solid temperature just prior to ignition. For a solid temperature of 21°C the pressure limit was 45 atm for pellets pressed from as-received powder of wide particle size range, 90 atm for pellets pressed from 75-105μ powder, and 100 atm for pellets of less than 53μ powder. When the pellets pressed from the as-received material were preheated to 70°C, the pressure limit was reduced to 20 atm, and when the solid was cooled to -18°C, no deflagration could be obtained at any pressure from 70 to 270 atm. In later work, Levy and Friedman (32), using a stronger ignition stimulus, found the deflagration pressure

limit to be 22 atm for pressed pellets at room temperature. Horton and Price (25) found this limit to be 3 atm when they cemented their pellets into their burner with an epoxy resin which was also used to inhibit the sides of the pellet and 23 atm when the pellets were pressed into metal sleeves. They attributed the lower result to the small amount of fuel the epoxy supplied at the burning boundary. For AP single crystals Hightower and Price (23) found the pressure limit to be 19 atm. These results indicate that this "go - no go" ignition procedure for determining the minimum pressure for deflagration is a slow and laborious experimental procedure which requires very careful measurements to obtain accurate results.

Woolderidge, Marxman, and Capener (57) used slow depressurization (about 0.7 psi/sec) to determine the pressure limit for composite propellants of various compositions. As depressurization proceeded, a photocell indicated the point of extinguishment. This technique appears best suited for propellants which burn very slowly (about 0.03 cm/sec in the cited work) near the limiting pressure since this allows the depressurization to proceed slowly enough to keep the burning process essentially at steady state. Results of the application of this technique to pure AP, which burns at about 0.3 cm/sec near the deflagration pressure limit, have not been reported.

The results of Friedman et al. (15) indicate that the strong dependence of the pressure limit on the solid

temperature can be utilized to determine the pressure limit. In the present work a linear temperature gradient was imposed along the length of an AP single crystal or pellet and the pressure of nitrogen or helium was adjusted so that the warm end of the AP would deflagrate but the cool end would not. Then the warmer end was ignited and the deflagration wave proceeded to a point where the solid temperature was too low for the deflagration wave to propagate at the existing ambient pressure. The length remaining unburned allowed the computation of the limiting solid temperature corresponding to the set pressure (Fig. II-1).

Experimental Apparatus

The temperature gradient of 10 to 20°C/cm along the length of the pellet or crystal was maintained by heating one end electrically with a Chromel ignition wire and by refrigerating the other end. The refrigerant was recirculated through a tube which was inserted through the end plate into the combustion chamber (described in Appendix A). This tube served as a mounting for the AP crystal or pellet (Fig. II-2).

Thirty-gauge Alumel-Chromel thermocouples were mounted in a notch at the base of the pellet and in a hole drilled near the heated end (Fig. II-2). Since it was not possible to drill holes into the single crystals without cracking then, a small section of a pressed pellet was glued to the heated end of all the single crystals and

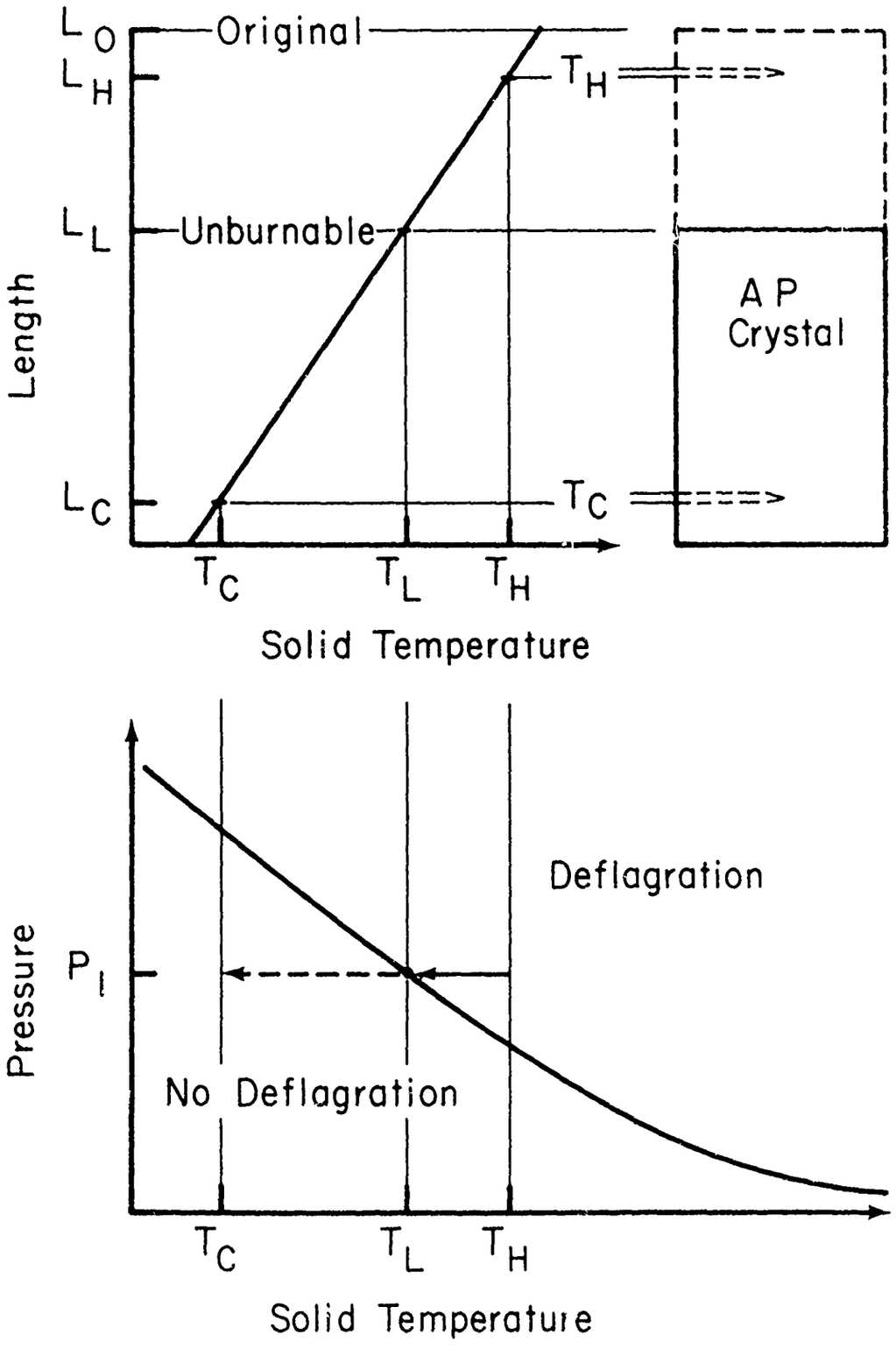

Fig. II-1. Measurement of limiting solid temperature, T_L, for deflagration at pressure P_1.

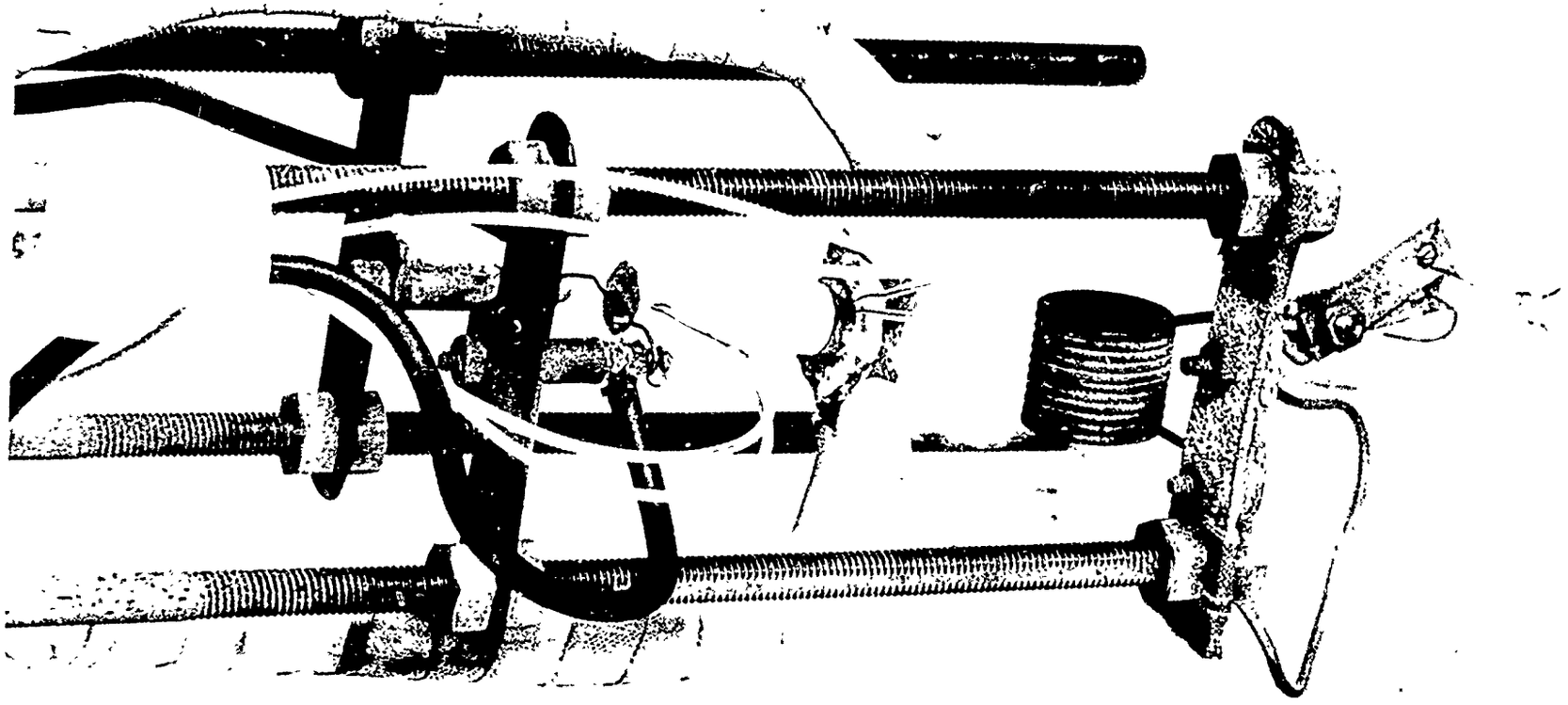

Figure II-2. Mounting of AP pellet for pressure limit measurement.

several of the pressed pellets and the thermocouple was mounted in this junction. These two techniques gave identical results since the burning continued at least 0.5 cm beyond the thermocouple at the heated end.

A piece of aluminum foil was glued over the entire heated end of the pellet to distribute the heat from the electrically heated Chromel wire as uniformly as possible (Fig. II-2). The current through this Chromel wire could be adjusted to heat the warmer end of the AP sample to a desirable temperature; then this same wire could be used to ignite the AP pellet. Since about 0.8 cm of the AP burned before the limiting conditions were reached, there was no effect of the aluminum foil or the glue.

A layer of glass wool about 3/4 inch thick was packed around the AP crystal or pellet as insulation thereby assuring a one-dimensional flow of heat along the axis of the sample and assuring a uniform temperature throughout any cross-section. The linearity of the temperature profile was verified by instrumenting a pellet with additional thermocouples on the centerline of the pellet and measuring the exact temperature profile. This insulation was attached to a spring which was held compressed by a short length of 30-gauge Chromel wire. Before ignition the Chromel wire was broken by passing an electric current through it, which in turn released the spring and pulled the insulation away from the AP. Figure II-2 shows the spring and insulation in the released position. If for any reason the insulation was not

removed, the expected deflagration pressure limits were not observed, possibly because the insulation retained the heat of combustion and heated the AP.

A 500-psig full-scale Heise gauge, accurate to 0.1% of full scale and calibrated on a dead-weight gauge, was used to measure the pressure.

Procedure

By adjusting the current to the heating wire and the amount of refrigeration, the temperature gradient along the length of the crystal or pellet was maintained at 10 to 20°C/cm at the proper temperature level for the set pressure. All samples were at least 2 cm in length and the pressure of nitrogen or helium was adjusted so that the AP would burn at least 0.5 cm beyond the thermocouple near the warmer end, but not as far as the thermocouple at the cooler end. When the temperature profile was steady for at least one-half hour the insulation around the AP was removed and the AP was ignited immediately. Since the pressure rise was as much as 5 to 10 psi, the peak pressure during the burning was recorded as the experimentally determined limiting deflagration pressure.

The length remaining after extinguishment was measured, and linear interpolation between the two thermocouple temperatures gave the limiting temperature corresponding to the measured pressure (Fig. II-1). The slight concave or convex shape of the extinguished surface indicated that the temperature was not exactly constant through the sample

cross-section; the length at the centerline was measured in all cases since this was the position of the thermocouples.

Discussion of Results

The resulting plot of the relationship between the limiting pressure and the solid temperature is presented in Fig. II-3, and the corresponding data in tabular form can be found in Appendix B. These data are fitted reasonably well by a straight line above 225 psia, and below this pressure the slope of the limiting pressure versus the solid temperature decreased considerably. The relatively high local temperatures near the heating wire at the warmer end of the AP crystal or pellet made it impractical to measure the deflagration limit above about 80°C because the AP would ignite prematurely. For this reason it was not possible to extend the data to atmospheric pressure where it has been reported (14,36) that AP will sustain a deflagration wave above about 270°C.

In contrast to the previous measurements of the AP pressure limit which depended upon a transient ignition process to determine a condition of steady-state deflagration, the present work utilizes an essentially steady-state process in this measurement. Since the solid reaction occurs essentially at the surface, the temperature profile in the solid during steady deflagration can be expressed as (9)

$$\frac{T - T_a}{T(0) - T_a} = e^{-x(u_s/\varkappa_s)} \qquad (1)$$

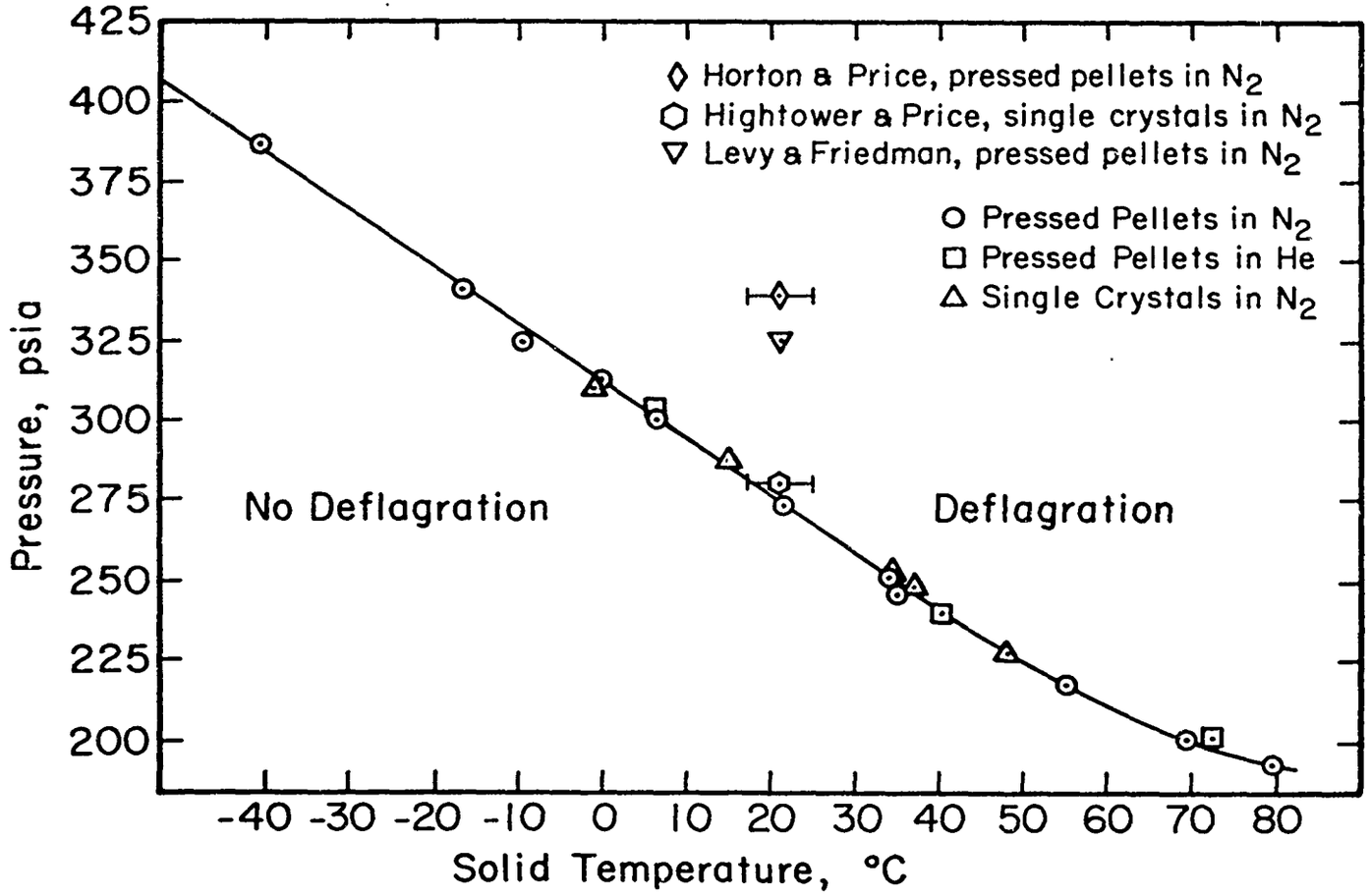

Fig. II-3. **Relationship between the limiting pressure and the solid temperature for the deflagration of ammonium perchlorate.**

where T indicates the solid temperature, x is the distance from the burning surface into the solid, the subscript a indicates conditions at $x = \infty$, u_s is the burning rate, and $\varkappa_s$ is the thermal diffusivity, $\lambda_s/\rho_s c_s$, which is about 0.001 cm^2/sec (40) for AP. Since AP burning rates are about 0.3 cm/sec at these low pressures, $\varkappa_s/u_s$ is about 0.003 cm. This implies that T is essentially T_a for x greater than 10 $(\varkappa_s/u_s)$ or about 0.03 cm. On this scale, the applied temperature gradient of 10 to 20°C/cm is negligible, and the burning process is essentially at steady state.

Although it might be expected that the pressurizing atmosphere plays a role in determining the pressure limit, substituting helium for nitrogen caused no detectable change in the pressure limit. This result is in agreement with AP burning rates which are the same in both nitrogen and helium (Chapter III).

The data in Fig. II-3 show that both AP single crystals and pressed pellets have the same pressure limit in contrast to the results of previous workers. Hence, this limit is a property of the ammonium perchlorate and is not influenced by interparticle processes in the pressed pellets. Considering the mounting evidence for a molten zone of AP at the burning surface (23), the result of a common pressure limit for crystals and pellets could possibly be explained by a molten surface zone.

Gaseous flames frequently exhibit a similar deflagration pressure limit which may be a function of composition,

and in some cases this limiting condition can be explained by heat losses (33). In a similar fashion, Levy and Friedman (32) have suggested that the low pressure deflagration pressure limit for AP could be caused by radiative heat loss. Since deflagration of AP on the inner cylindrical surface of an annular pressed pellet gave essentially the same pressure limit (25), it seems unlikely that radiation heat losses are important in determining the pressure limit. Furthermore, mathematical studies by Johnson and Nachbar (28) indicate that the heat loss necessary to arrive at the observed deflagration pressure limit could only be explained by introducing some heat loss considerably larger than that which could be reasonably explained on physical grounds. Thus it would appear that heat and mass transfer limitations within the flame zone must account for this limiting condition and also for the unstable steady state or ignition point which coincides with the deflagration steady state at the pressure limit. Since the thickness of the flame zone increases with decreasing pressure, it is conceivable under deflagration conditions that the heat flux from the flame zone to the solid decreases as the pressure is lowered because of the increased thickness of the flame zone. Since the overall deflagration process depends upon the feedback of heat from the flame zone to the solid to supply the energy necessary for the solid-phase reactions, it seems possible that below this pressure limit this relatively thick flame zone is unable to supply a sufficient amount of heat to the

solid to maintain deflagration. Therefore the present measurements of the unique condition where the unstable steady state or ignition point coincides exactly with the stable deflagration steady state must await a quantitative theory of ignition and deflagration for their explanation.

CHAPTER III

THE BURNING RATE OF SINGLE CRYSTALS OF AMMONIUM PERCHLORATE

Introduction

In characterizing the reactive stable steady state for AP above the deflagration pressure limit the burning rate of the solid has been measured by many laboratories [see Pittman's review (35)]. Since almost all of this work has been done at room temperature and because the determination of the pressure limit in Chapter II has shown that the effect of the ambient temperature is quite important, this section of this research program was concerned with the measurement of the burning rate of pure ammonium perchlorate over a wide range of pressures and temperatures. When pellets pressed from granulated AP are burned it has been shown that the rate is strongly influenced by the particle size of the AP powder (44,45,46) and it has been suggested that the ignition delay involved with each particle within the pellet can account for the change in burning rate with particle size (44,45). Since a theoretical explanation of AP deflagration must involve the correlation of these burning rate data with the fundamental chemical processes occurring during deflagration, the additional complexity of possible intercrystalline effects was avoided by burning large single crystals of ammonium perchlorate.

Other laboratories have also grown AP single crystals

for deflagration studies. The results of Whittaker and Barham (55) were not definitive because a small amount of polygalacturonic acid was used to modify the habit of the AP crystals. The work of Hackman and Beachell (19) appeared to agree well with that of Hightower and Price (23), but data at only two pressures were reported. Engleman's burning rate data (10) were considerably higher than those of Hightower and Price (23). In the present work Engleman's (10) hot gas ignition apparatus was compared with a hot wire ignition apparatus very similar to that of Hightower and Price (23) in the same combustion chamber, and it was apparent that the hot gas ignition apparatus affected the burning process. This preliminary investigation indicated the possibility that the burning rate increased because the gas oven in the ignition apparatus caused the hot reaction products to recirculate back into the flame zone. (The details of this investigation are presented in Appendix C.) Since there was no indication that the wire used in the hot wire ignition apparatus interfered with the deflagration process, this ignition procedure was used in the present work.

Since the agreement on experimental data taken at different laboratories is extremely important in the determination of an intrinsic burning rate for ammonium perchlorate, AP single crystals were exchanged with J. D. Hightower and T. L. Boggs at the Naval Weapons Center (NWC) in China Lake, California, to test whether the difference in apparatus

had an effect on the measured burning rates. Consequently a second objective of this research, in addition to taking deflagration data over a wide range of pressures and temperatures, was to compare the data taken on samples of the crystals grown at the University of California (U.C.), Berkeley, and on samples of crystals grown at the Naval Weapons Center when burned at the Naval Weapons Center and when burned at the University of California, Berkeley.

Experimental Technique

High-speed motion photography was used to measure the AP burning rates. The crystals were mounted between two opposing windows in a high-pressure combustion chamber which was pressurized with either nitrogen or helium. One window was used for the light source and the other for the camera (Fig. III-1); hence the technique resembles shadow photography. Figure III-2 shows another view of the combustion chamber and the camera in position to photograph the title board prior to an experimental run; the camera could be rotated and locked into the position shown in Fig. III-1 for for photographing the burning. The crystal was mounted to burn either normal to the m, [210], face or normal to the c, [001], face, and the crystal was ignited by electrically heating a Chromel wire pressed against the desired face of the crystal (Fig. III-3). The crystals were usually about 1.5 cm in length and about 0.4 cm on each side.

As indicated by the sample frames in Fig. III-4, the movies were clear and unobstructed by smoke; hence no gas

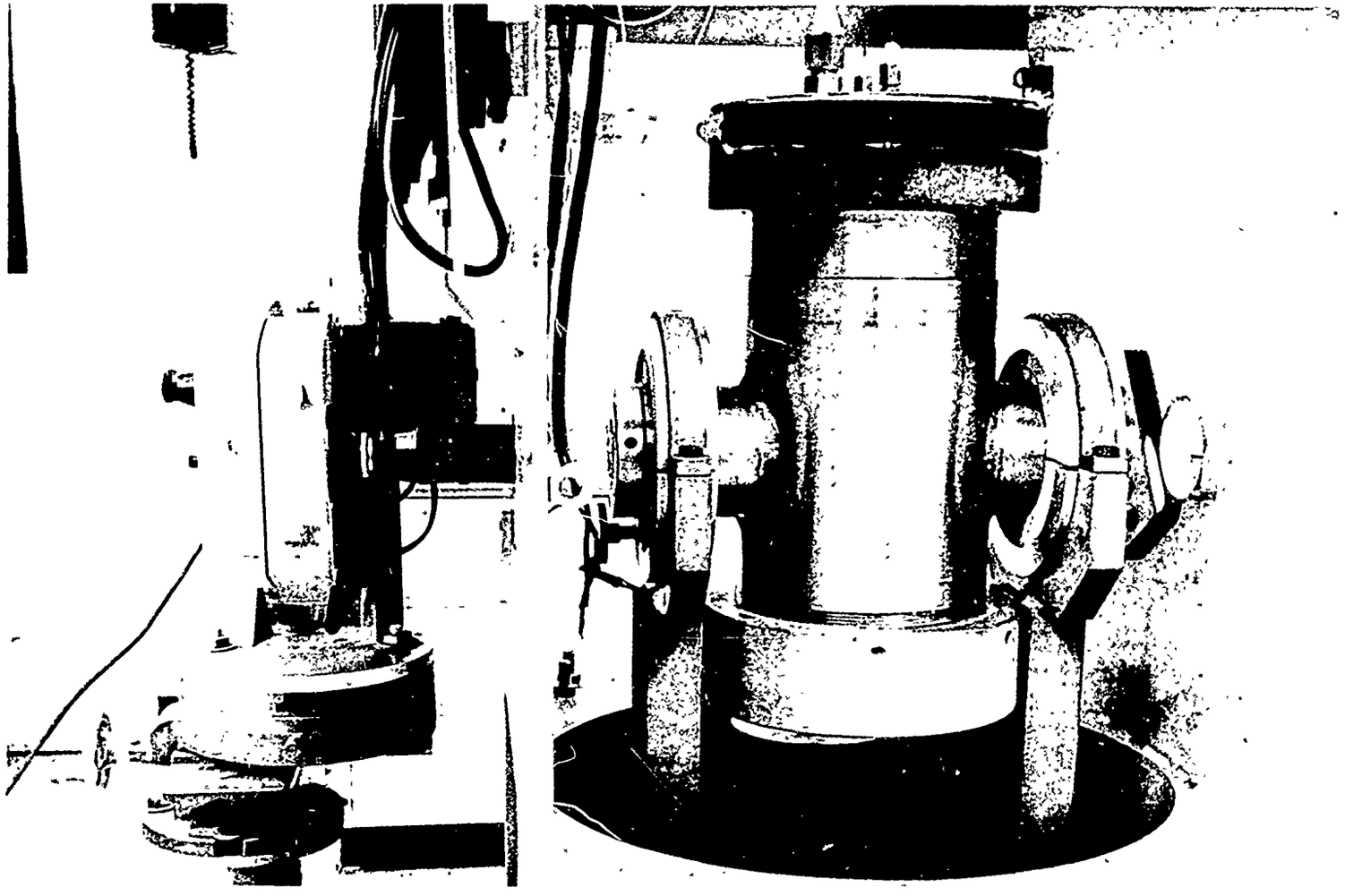

Figure III-1. Combustion chamber and high speed movie camera.

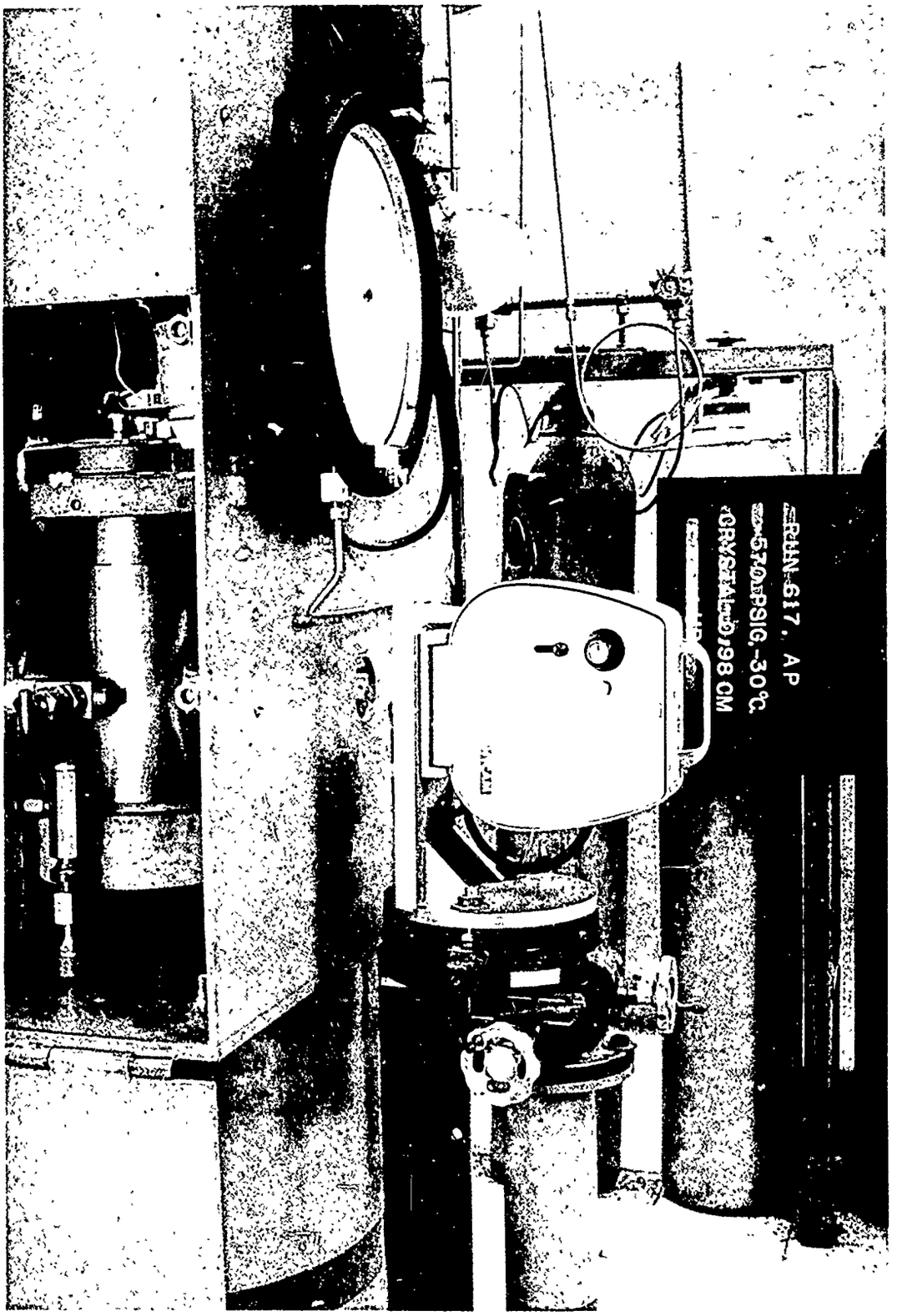

Figure III-2. Combustion chamber, high speed movie camera, and titling board.

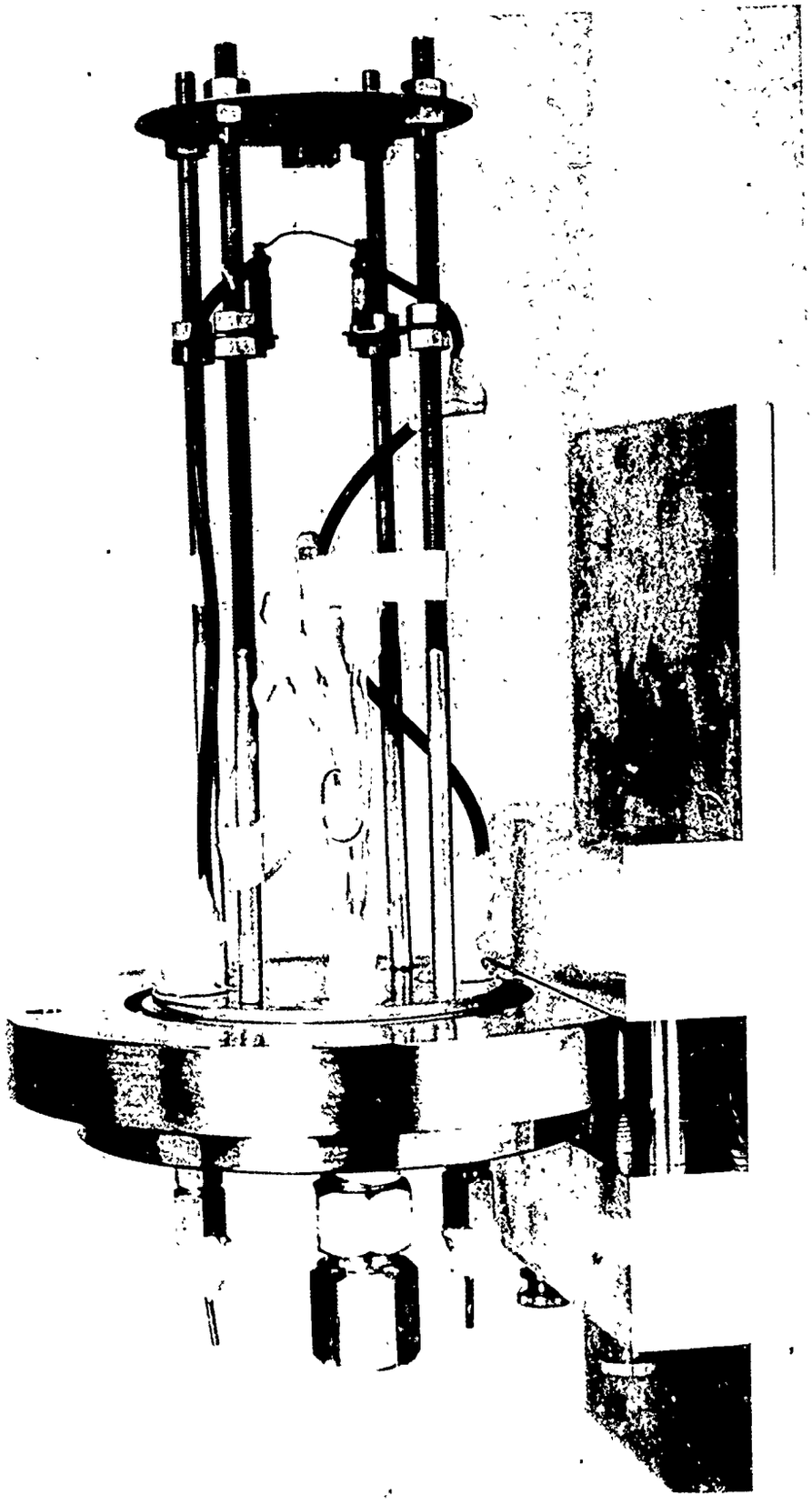

Figure III-3. Crystal mounting for hot wire ignition.

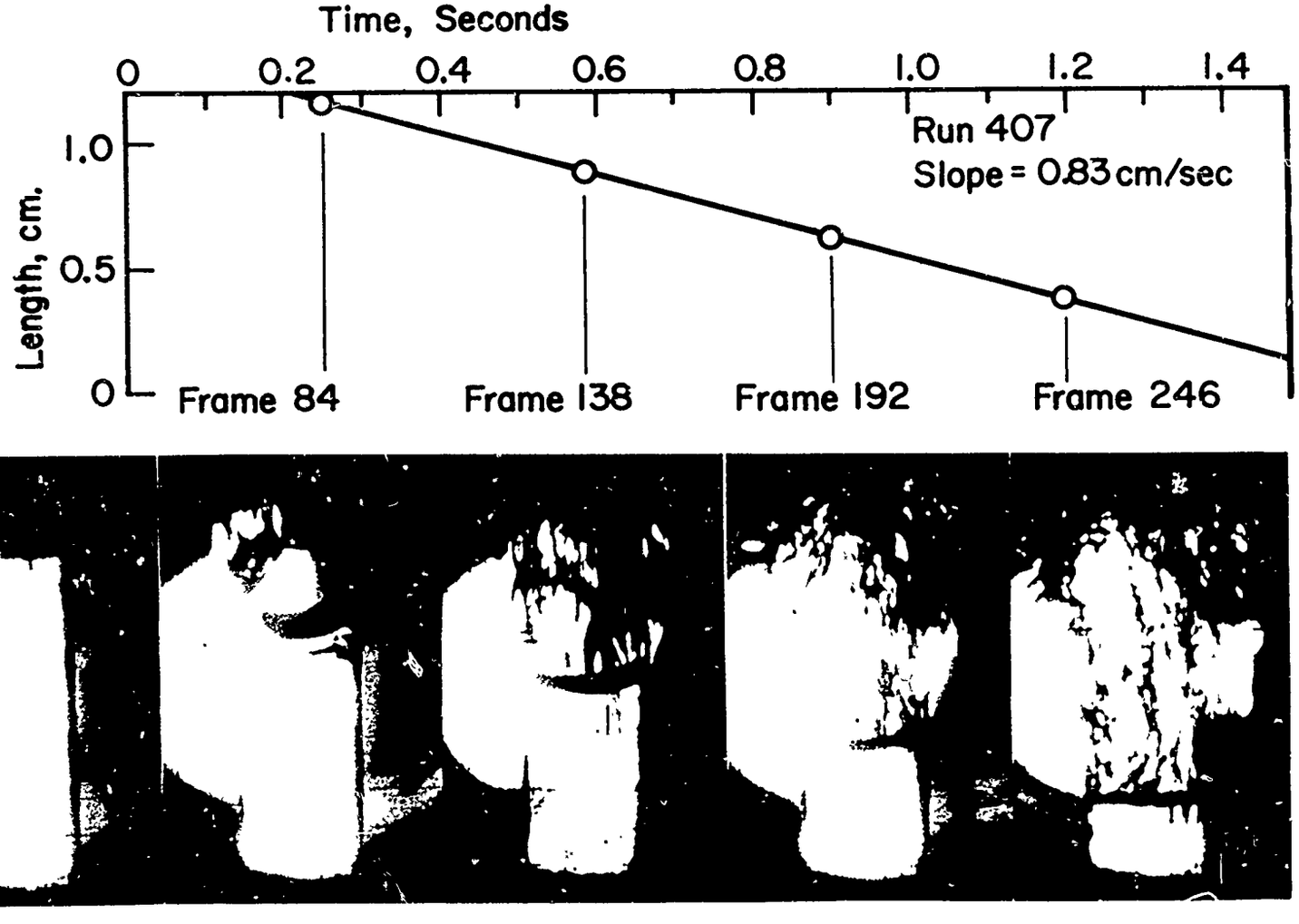

Figure III-4. Sample movie frames showing deflagration rate of AP single crystal.

purge was necessary. The camera was operated at about 200 frames per second with timing marks every 1/120 second to give ample data for a thorough statistical analysis. In taking measurements from the projected movies no data were taken until the deflagration was clearly stable after the ignition transient and until the burning surface had proceeded well beyond the ignition wire as indicated by the second frame in Fig. III-4. About 20 length-versus-time data points were recorded and fitted to a straight line using a least squares digital computer routine. On most runs the variance σ^2 of this length-versus-time fit was about 0.001 cm^2. Since the time was known very accurately, the measured burning rate had a standard deviation of about 0.01 cm/sec.

These data were also fitted to a second-order polynomial to test the linearity of the burning. The F statistic (49), in this case the ratio of the variance of the fit by the first-order polynomial to the variance using the second-order polynomial, was computed. The F test indicates that for F values less than about 3 the second-order coefficient cannot be distinguished from zero with 95% confidence; i.e., the burning is linear within the accuracy of the data (47). A vast majority of the runs indicated a constant burning rate by this test; the remainder frequently showed considerable cracking of the crystal during the burning and were discarded. A complete discussion of the data analysis is given with the data in Appendix B.

A preliminary estimate of the burning rate could be

made from the output of the photocell shown in Fig. III-3. The length of the crystal was divided by the total burning time indicated by the photocell on an oscillograph to give a measure of the burning rate. This method was only approximate since the transients occurring immediately after ignition could not be avoided.

Discussion of Results with U.C. Crystals

The Burning Rate at Constant Ambient Temperature

Figure III-5a presents the AP single crystal burning rate data from near the pressure limit to 5000 psia, the limit of the apparatus, at ambient temperatures of 89, 23, and -28°C. Most points are averages of at least two runs, and the experimental data used to construct these curves are presented in Table B-1. At many conditions, particularly those defining the predominant peak in the burning rate isotherms, several identical runs were made and the reproducibility appeared to be excellent.

As shown in Fig. III-5b the initial rise of the burning rate with pressure at 23 and 89°C was essentially linear. Summerfield (52) has shown that such a linear relationship between burning rate and pressure is reasonable for AP composite propellants at low pressures where the flame could be considered premixed. [At higher pressures diffusion was shown to be important in the burning of the composite propellants, and the burning rate was shown to be proportional to the one-third power of the chamber pressure

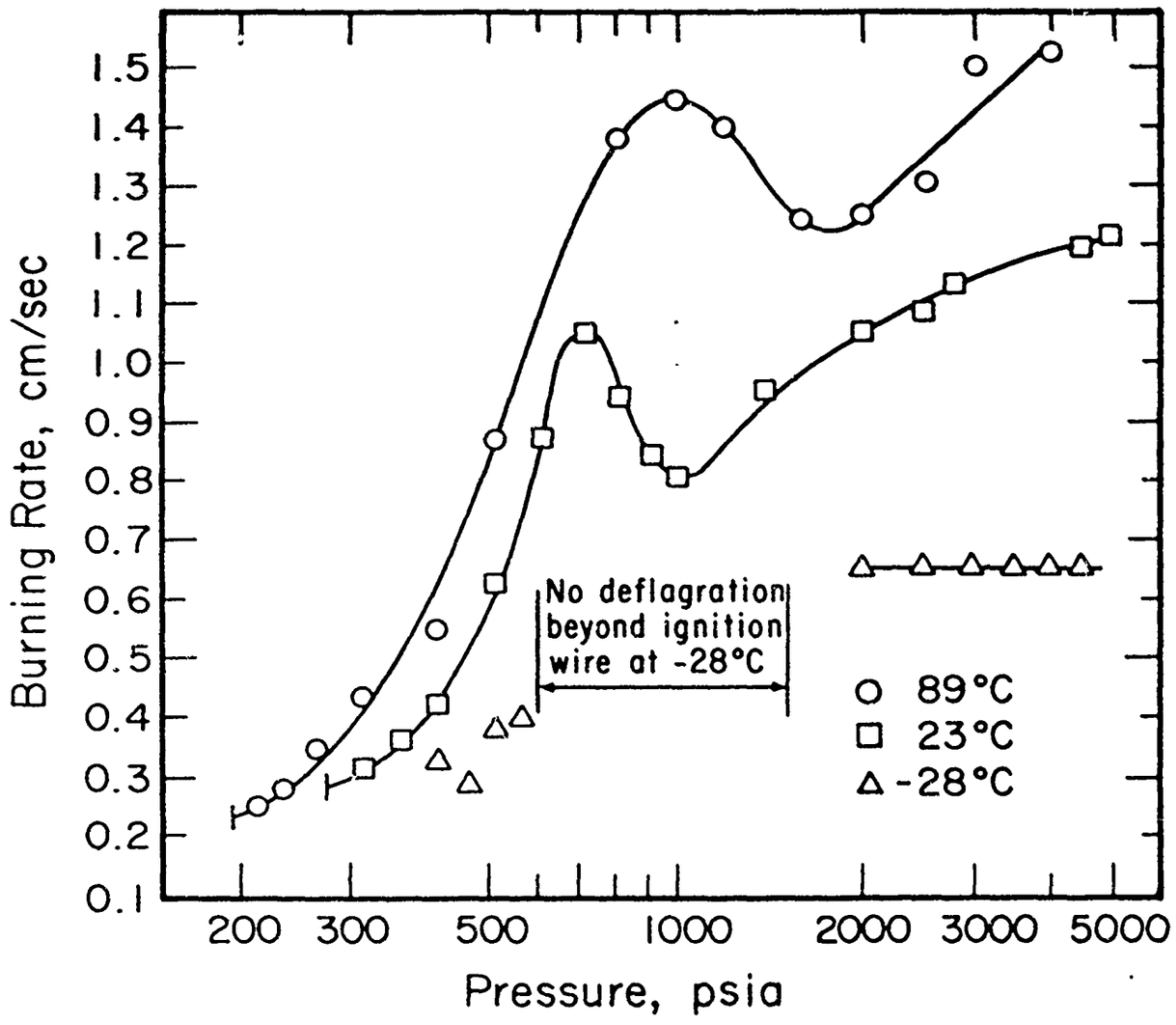

Fig. III-5a. Burning rates of AP single crystals at constant ambient temperature.

(52).] Linear extrapolation of the burning rate data (Fig. III-5b) to the pressure limit indicates that the burning rate does not approach zero as the pressure limit is approached. At both 23 and 89°C the burning rate extrapolated to the pressure limit is about 2 cm/sec. This discontinuity in the burning rate isotherm can be understood in terms of the qualitative discussion in Chapter I from which it should be clear that the pressure limit generally occurs at finite burning velocity.

The consistent shape of the burning rate isotherms in Fig. III-5a suggested that, as the temperature was lowered, the entire shape of the burning rate isotherm was compressed within a narrower range of pressures. This ambient temperature effect is seen most clearly in the -28°C isotherm which is horizontal between 2000 and 4500 psia and which appeared to approach a high-pressure asymptote in this region. Although this high-pressure asymptote was not found at higher temperatures, this trend could be discerned. Since these data offer insight into the scaling of pressure and temperature they should be very helpful in the formulation and evaluation of theories of AP deflagration.

From the curves in Fig. III-5a it seems likely that the mechanism of AP deflagration changed as the pressure was increased and that this change in mechanism could explain the peak in each burning-rate isotherm. Since only very approximate models have been considered for the burning process, this possibility of a changing mechanism presents

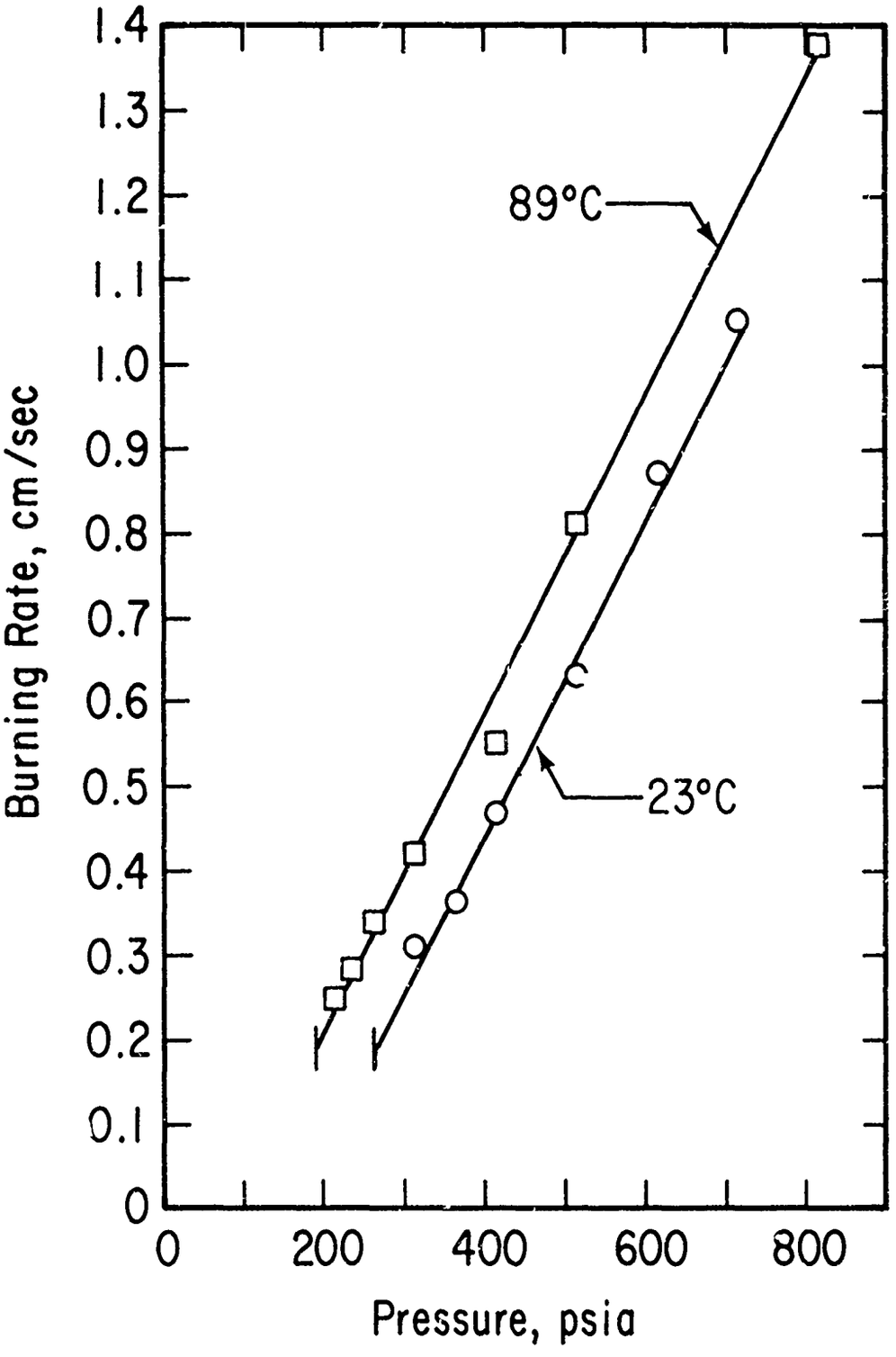

Fig. III-5b. AP single crystal burning rates: region of linear increase with pressure.

a distinct challenge to the further understanding of AP deflagration. From Fig. III-5a it is clear that as the ambient temperature is decreased the transition from the low pressure mechanism to the high pressure mechanism occurs at lower pressures. In addition, there were significant preliminary indications that the high pressure deflagration mechanism had a distinct pressure limit analogous to the deflagration pressure limit found for the low pressure mechanism in Chapter II. At -28°C between about 600 and 1500 psia the movies showed that ignition took place but that the deflagration did not proceed beyond the region preheated by the hot ignition wire. Between 415 and 565 psia at -28°C the crystals could be ignited by the standard hot wire procedure although the ignition delay was long, a characteristic of ignition near the pressure limit at all the temperatures studied. The movies indicated that during this ignition delay the hot ignition wire penetrated into the crystal; the reactions spread slowly across the ignited surface with the development of an apparent froth; then the deflagration process predominated and the burning interface propagated through the solid. Since the scale is quite compressed at this low temperature, the few data at -28°C between 415 and 565 psia did not justify drawing the complete isotherm in this region, and more data will be necessary to elucidate these interesting conditions. Between 2000 psia and 4500 psia at -28°C the ignition and deflagration appeared to be quite normal although the burning rate

did not change in this pressure range. Since the apparent discontinuity in the -28°C isotherm was not clearly delineated experimentally, it cannot be concluded that deflagration is impossible in this range of pressures; however it is clear that if deflagration is possible it is considerably more difficult to establish a deflagration wave which will propagate unassisted through the solid. This apparent pressure limit for the high pressure deflagration mechanism may possibly explain the high pressure limit found by Friedman et al. (15) for AP pellets. It is also quite interesting to note that an interpolation across the discontinuity in the -28°C isotherm (Fig. III-5a) is considerably above about 0.3 cm/sec which was about the minimum measured burning rate at -28°C for the low pressure mechanism; this seemed to imply that the apparent pressure limit for the high pressure mechanism occurred at a distinctly higher burning rate than for the low pressure mechanism. Hence, although the apparent discontinuity in the -28°C burning rate isotherm seemed to be similar to the deflagration pressure limit discussed in Chapter II, it appeared to be a different mechanism.

Since a definitive experiment is necessary to delineate a discontinuity in a burning rate isotherm, preliminary efforts were made to apply the experimental technique presented in Chapter II to measure the limiting solid temperature for deflagration in the region of pressures between about 600 and 1500 psia. At a pressure of about

1000 psia the warmer end of the crystal was held at about 0°C and the cooler end near -30°C for three runs. (The data are presented in Table B-6.) As was done previously, a section of a pressed pellet was glued to the heated end of the crystal to hold the thermocouple. In these experiments, in contrast to those measuring the low pressure deflagration limit, the crystal failed to ignite after the pellet section had burned. At 800 psia the crystal likewise failed to ignite when the warm end was at -21°C, but when the two thermocouple temperatures were -5 and -31°C the crystal ignited and burned entirely. Certainly no definite conclusions can be drawn from these preliminary data; yet it seems apparent that there is a different character to the deflagration and ignition of AP under these conditions and further research in this region of conditions could be very informative.

The Burning Rate at Constant Pressure

Since the dependence of the AP burning rate on the ambient temperature is not completely explicit in the semi-log plot of Fig. III-5a, a cross-plot of this relationship at various pressures is shown in Fig. III-6. The burning rate increased non-linearly with the ambient temperature, and the slope and non-linearity both increased with the pressure. Shannon and Petersen (45) reported the variation in the burning rate of pressed pellets of AP with the ambient temperature over a limited range of pressures; their

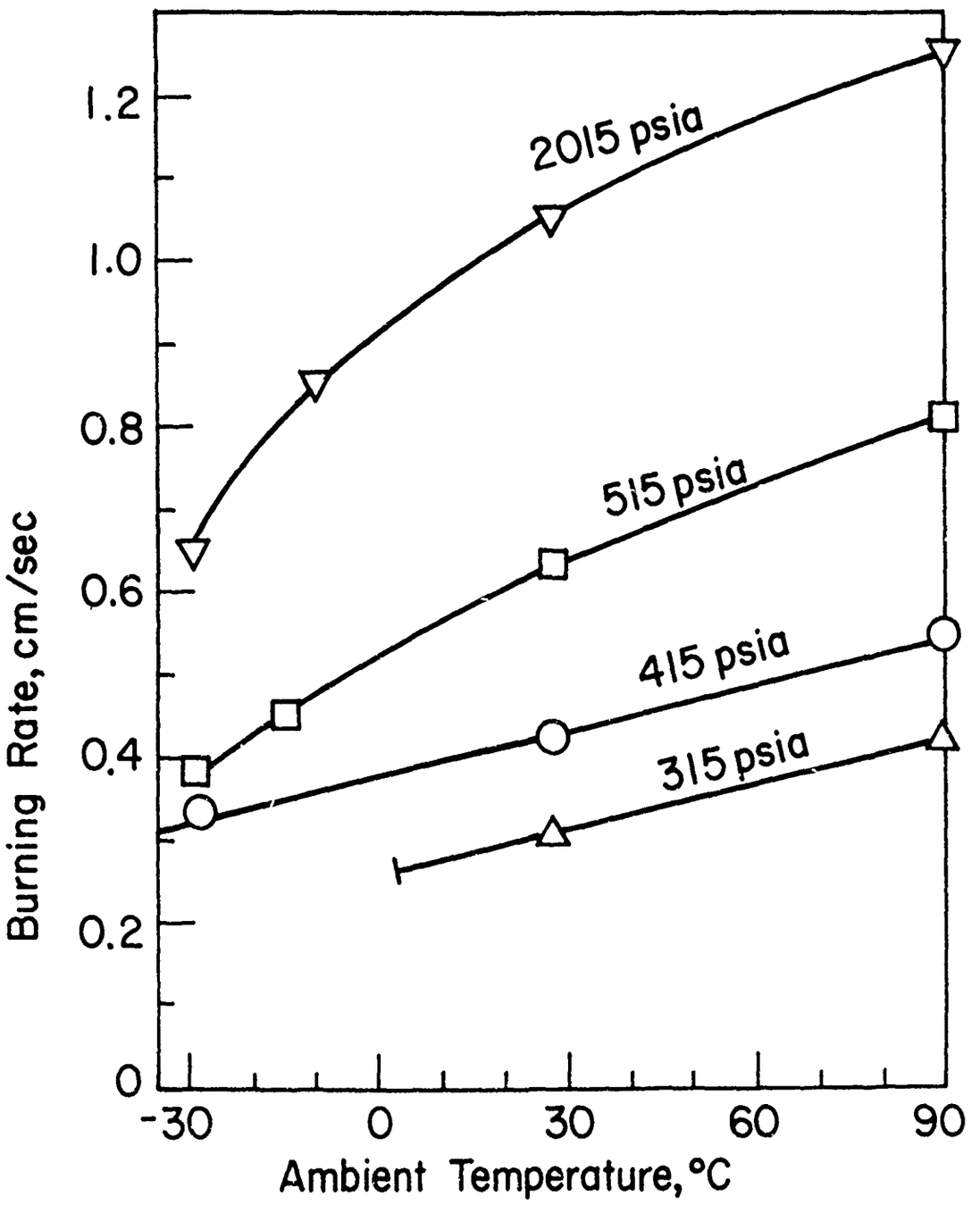

Fig. III-6. Burning rates of AP single crystals at constant pressure.

results showed general agreement, but their small range of pressures made a complete comparison impossible.

In addition to measuring the burning rate at different ambient temperatures, a few preliminary runs were made to measure burning rate versus ambient temperature on a single experiment by imposing a temperature gradient along the length of the crystal. In Chapter II this procedure was used to determine the deflagration pressure limit as a function of the solid temperature, and Chapter II gives the details of the apparatus, procedure, and results. The extension of this procedure to measuring the burning rate as a function of the solid temperature is straightforward, but not simple in practice. The applied temperature gradient was linear and was measured by thermocouples at each end of the crystal, and the photographic record gave the normal data for length versus time. A second-order polynomial was fitted to these data and differentiated to give burning rate versus solid temperature as shown, for example, by run 599 in Fig. III-7. Differentiation of such a fitted polynomial tends to exaggerate the differences near the ends of the interval even though the average value over the interval is accurate as shown in Fig. III-7. In addition, experimental problems were encountered when the modifications used to apply the temperature gradient caused the optically dense reaction products to obscure the burning interface, making photographic analysis impossible. Only a very few runs were made using this

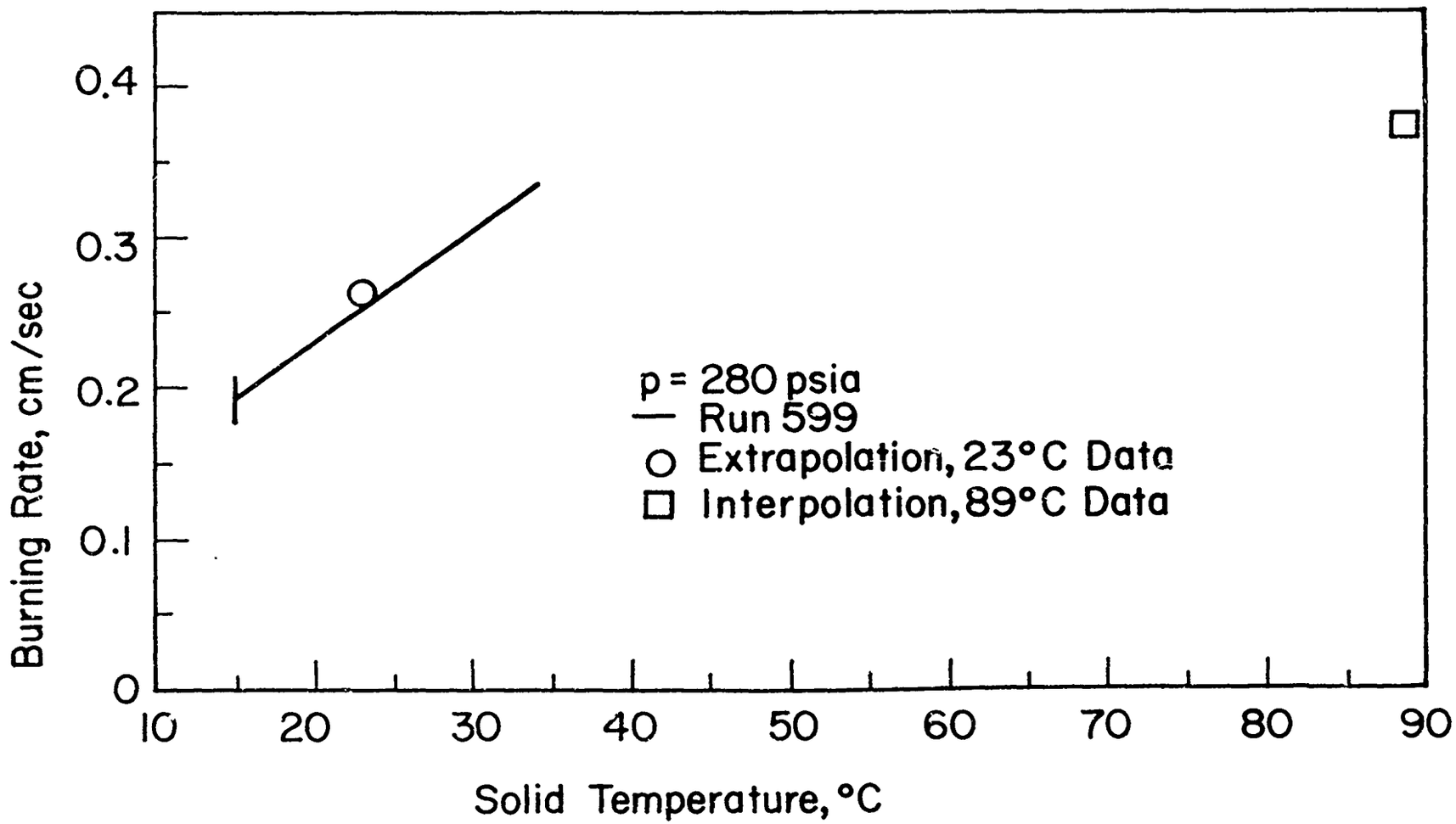

Fig. III-7. Analysis of burning of an AP crystal with an imposed temperature gradient.

technique, but they offered the promise of generating a considerable amount of data with relatively few experiments. Careful design of the apparatus should permit photographic analysis throughout the entire burning, and by using longer crystals and applying a larger temperature gradient the statistical determination of the change in burning rate with temperature should be significantly improved. Of particular interest will be the burning rate as the solid temperature approaches the limiting temperature for deflagration (Fig. III-7); determination of this limiting rate over a wide range of pressures could shed new light on this quenching process.

The Relationship Between the Pressure and the Ambient Temperature for Constant AP Burning Rate

This chapter has been concerned with the relationship between AP burning rates, the pressure, and the ambient temperature, and two different representations of these data have been presented in Fig. III-5a and Fig. III-6. In Fig. III-8 a third possible cross-plot is presented of the pressure versus ambient temperature for conditions of constant burning rate. Included also on this figure is the deflagration pressure limit curve presented earlier in Fig. II-3. Although there are insufficient data on this figure to define the constant burning rate contours exactly, the dashed lines have been drawn to show the striking parallelism between the constant rate contours and the deflagration

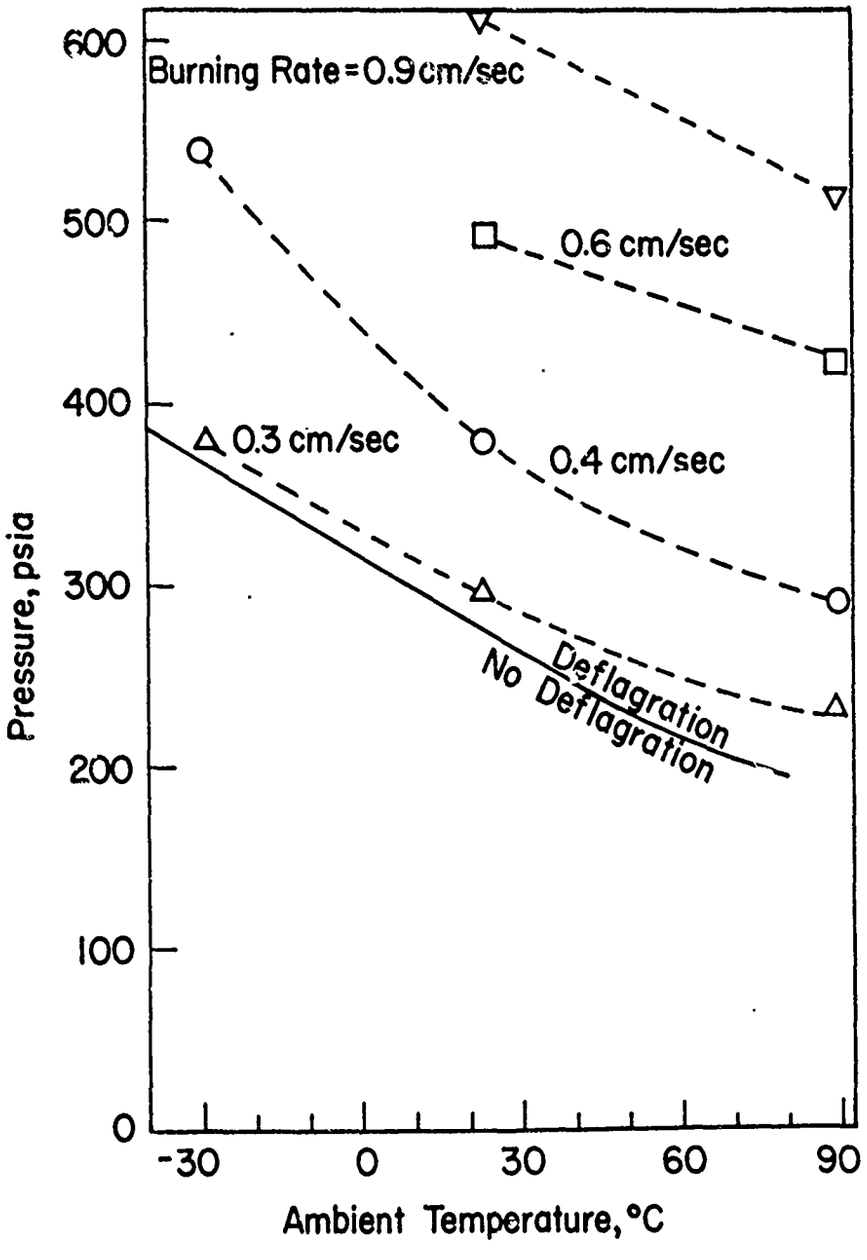

Fig. III-8. The relationship between the pressure and the ambient temperature for constant burning rates for AP single crystals.

pressure limit. This graph suggests the possibility that the limiting conditions for deflagration occur at a fixed burning rate and that AP deflagration does not occur at rates significantly below 0.2 cm/sec. This would then tend to suggest that a different mechanism is involved in the deflagration process reported by Friedman and Levy (14) to occur at one atmosphere and 267°C with a burning rate of 0.029 cm/sec, and a different mechanism seems plausible since AP decomposes spontaneously at such a high temperature.

In most models of AP deflagration it is postulated that the burning rate is a function only of the surface temperature and that it is the balance between the various possible exothermic and endothermic processes which determines this surface temperature and, hence, the burning rate. It seems entirely conceivable, then, that the contours of constant burning rate in a plot such as Fig. III-8 are equivalent to contours of constant surface temperature. A significant obstacle in relating burning rate data to a theory for deflagration is that the temperature of the burning surface is not measured simultaneously, in general, and that this surface temperature is not known with sufficient accuracy to evaluate a theory of deflagration. It appears that this problem can be avoided by comparing the theoretical conditions of constant burning rate with the data presented in a graph such as Fig. III-8.

As an example, consider the assumption that the burning rate of a pure single crystal is determined solely

by the burning surface temperature. In the qualitative description of deflagration given in Fig. I-1, the constant burning rate contours of Fig. III-8 would be represented by deflagration ("D") intersections falling on vertical lines in Fig. I-1. If the pressure limit does occur at a constant burning rate, then in Fig. I-1 all points of Q_F--Q_B tangency such as I_1,D_1 and I_3',D_3' would also fall on a vertical line. By continuing this analysis a step further it is seen that changes in Q_B on a vertical line in Fig. I-1 can be simply calculated as minus the product of the solid heat capacity and the difference between the two ambient temperatures. Since at steady state $Q_B = Q_F$, the calculated change in Q_B for the given change in the ambient temperature is identical to the change in Q_F for the corresponding change in pressure. As it is quite conceivable that the surface reactions depend only on the surface temperature and are independent of pressure, these calculated changes in Q_F would be equivalent to changes in Q_G, the heat flux from the gas-phase reactions back to the solid surface, for the same change in pressure. This reasoning is illustrated in Fig. III-9 for the hypothesis that the pressure limit occurs at a constant burning rate and constant surface temperature and for the assumption that the surface reactions can be adequately described by a zero-order Arrhenius rate expression. The qualitative theory of deflagration given in Chapter V gives essentially the same description of

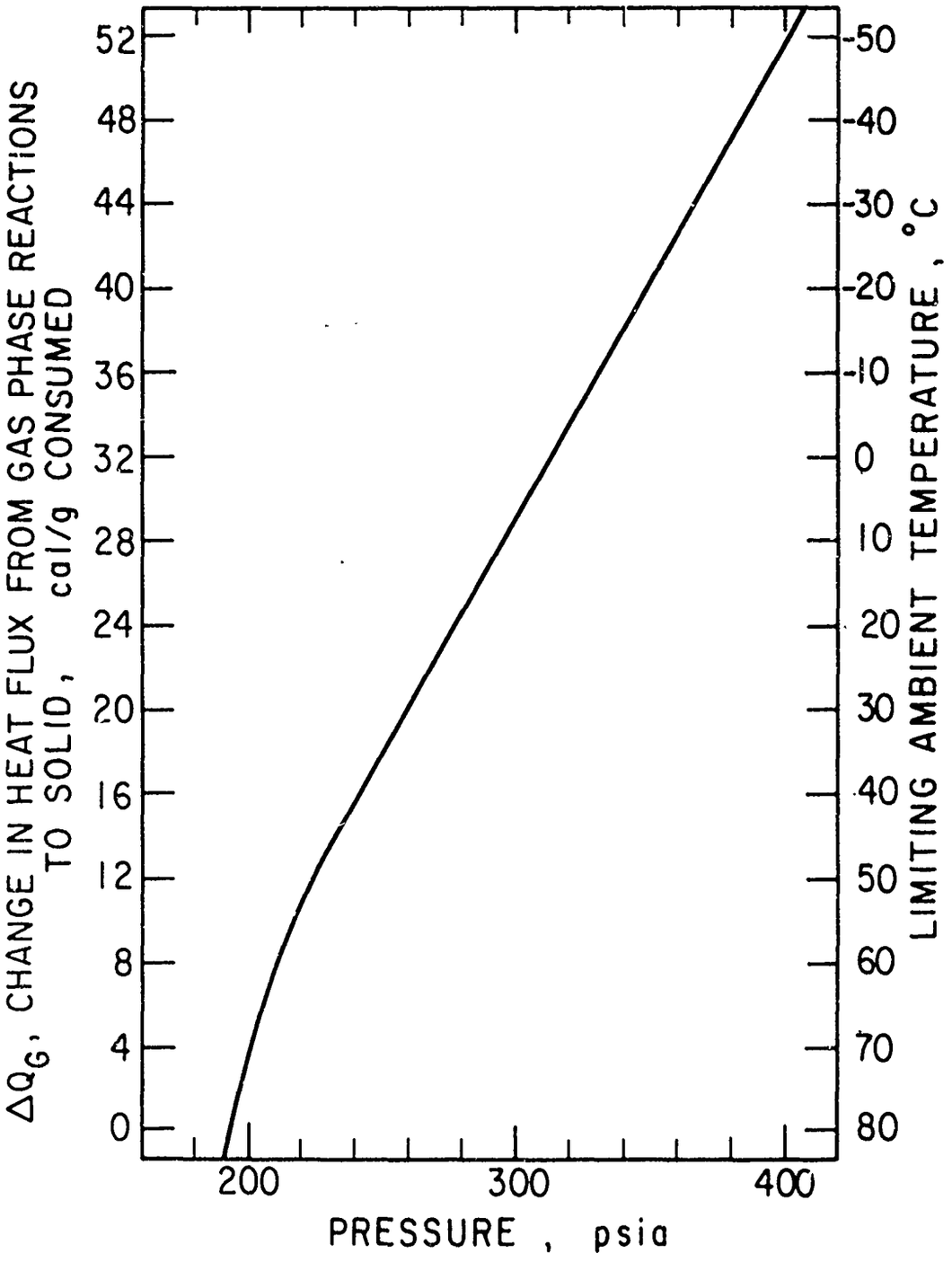

Fig. III-9. The change in heat flux from the gas-phase reactions to the solid surface with changing pressure at the deflagration pressure limit.

stable deflagration as the theory of Johnson and Nachbar (29) and indicates that Q_G should be proportional to pressure. Thus this theory is at least qualitatively supported by the data in Fig. III-9 at pressures above about 225 psia. The other contours of constant burning rate could also be compared with theoretical predictions when sufficient data are available. From this example it seems clear that comparing constant burning rate data with theoretical predictions is quite important because entirely different aspects of the theory are tested than when constant ambient temperature data are used. In the cited example the predicted linearity of Q_G with pressure could be studied without assigning values to the many parameters in the model. Hence further work to obtain constant pressure data over a wide range of pressures and temperatures offers the promise of great interest and utility.

The Effects of Orientation and of Pressurizing Gas on AP Deflagration

Since the combustion chamber could be rotated about the axis of the windows, the crystals could be oriented so that the burning surface receded downwards, horizontally, or upwards to observe any effects of natural convection on the burning rate. No difference could be detected between those runs in which the burning interface receded downwards and those in which the surface receded horizontally, and, consequently, all these data have been averaged together in Fig. III-5. (Table B-3 indicates the orientation of the

combustion chamber.) Burning was generally done with the surface receding downwards since good visibility was slightly more consistent in this orientation. When the combustion chamber was turned so that the burning surface receded upwards, it was impossible to observe the burning interface because of the optical distortion caused by the dark, hot reaction products rising around the crystal. The estimate of the total burning time given by the photocell indicated that the burning was significantly faster in this orientation; this was quite possibly caused by the feedback of heat and reactive species into the flame zone. For this reason no data were taken with the burning surface receding upward, and vertical burning is henceforth used to refer to the orientation with the burning surface receding downward. The fact that the burning rate was the same with the surface receding horizontally or downwards reinforced the assumption that natural convection did not influence the deflagration process.

In addition to the standard pressurization with nitrogen, on seven runs helium was used and the burning rates agreed very closely with those obtained in nitrogen. These helium data (Table B-3) clearly defined the whole structure of the room temperature burning rate isotherm and have been averaged into the data shown in Fig. III-5. One might expect that, if the pressurization gas was involved in the deflagration process, the difference in physical properties, such as the thermal conductivity and mass diffusivity,

between nitrogen and helium would affect the burning rate. Since nearly all deflagration theories assume that all gas-phase species have the same physical properties, there is no way to estimate the order of magnitude of the difference in burning rate one could expect with changes in the pressurizing gas. From the burning rate data it appears that if there is a difference in burning rate when helium is used for pressurization instead of nitrogen this difference is quite small. Although one could not conclude from this result that the pressurization gas played no role in determining the deflagration rate, the influence of the inert environment was not significantly affected by a considerable change in pressurizing gas. This result together with the result that natural convection was unimportant tended to support the premise that the measured burning rate was truly characteristic of ammonium perchlorate.

The rate of crystal growth was generally fastest perpendicular to the [210] face, and hence most crystals were burned along this crystallographic axis. As in the work of Whittaker and Barham (55) and Hightower and Price (23) there was no detectable difference in burning rate along the different crystallographic axes, either [001] or [210]. Frequently, when a crystal was ignited on the [210] face, the burning interface developed as the [110] face, which was perpendicular to the sides of the crystal and presented the minimum burning surface area. The burning rate was always measured perpendicular to the burning surface and

appeared to be independent of the crystallographic axis. In addition, the 15° angle between the [210] and the [110] axes is too small to have an appreciable effect on the measurement of the burning rates. The increasing evidence (7,23,39) for a molten zone of AP at the burning surface may explain this observation that the AP burning rate is independent of the crystallographic axis and strictly characteristic of the ammonium perchlorate.

Discussion of Results with NWC Crystals

As mentioned in the introduction to this chapter, AP single crystals were exchanged with Hightower and Boggs at the Naval Weapons Center (NWC) in China Lake, California, to test whether differences in apparatus had an effect on the measured burning rates. The comparison of the four possible combinations of the two crystal sources and the two locations for burning is given in Fig. III-10. When the crystals grown at the University of California, Berkeley, were burned at the Naval Weapons Center, the height of the peak in the burning rate isotherm increased somewhat and seemed to shift from a maximum at 700 psia to a maximum at about 1000 psia (8). When the crystals grown at the Naval Weapons Center were burned at the University of California the agreement with the data from NWC was remarkable. However, in this case, the exact location and height of the peak in the burning rate isotherm was not determined with sufficient data points to show complete agreement between the two sets

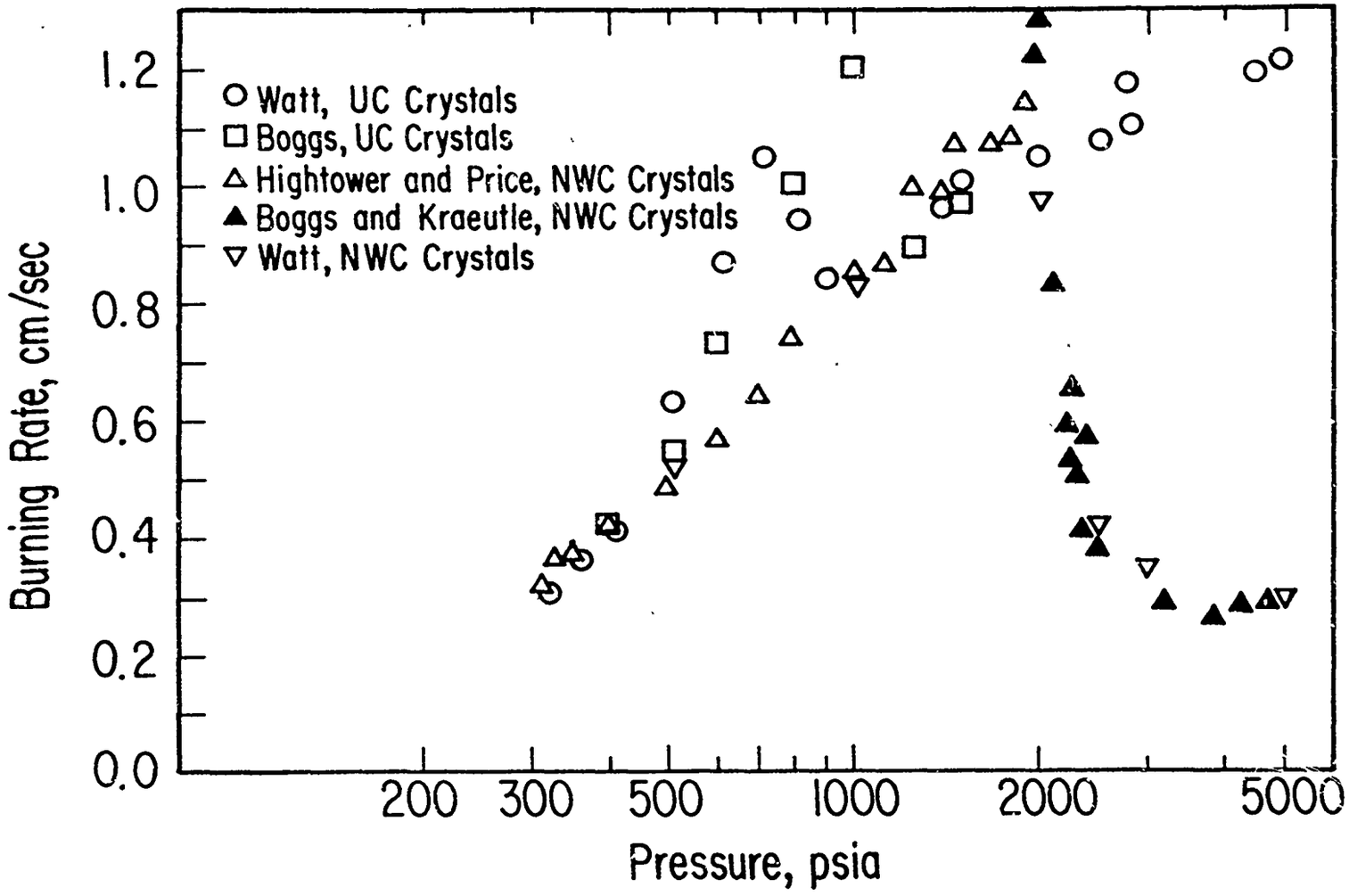

Fig. III-10. Comparison of room temperature burning rates of AP single crystals grown at U.C. and at NWC.

of data. The NWC data has been reported in several publications (7,23,39) but the most complete discussion of the data is given in reference 7.

From these comparisons there appeared to be a slight effect of apparatus on the burning rate, and further investigation will be necessary to test this hypothesis. The only apparent difference in apparatus was that at NWC nitrogen was flowed past the crystal to purge the reaction products from the system in order to improve the photography (39). It is interesting to note that the agreement between the data taken at NWC and at UC was excellent except at the peak in the burning rate isotherm. If the deflagration mechanism changes near this peak, it may be conceivable that the slight differences in apparatus only affected the balance of the two mechanisms in the region where neither one was dominant. Clearly, though, the apparatus did not alter the basic shape of the burning rate isotherms, and this was most significant since it is the basic shape of this curve which a theory of AP deflagration must endeavor to explain.

Comparison of Burning Rates for AP Single Crystals and Pressed Pellets

Since large single crystals of ammonium perchlorate were used in this research program to avoid possible interparticle effects involved in the deflagration of pressed pellets of AP powder, a brief comparison of the burning rates of the single crystals and the pressed pellets is presented in Fig. III-11. The general agreement between the data of

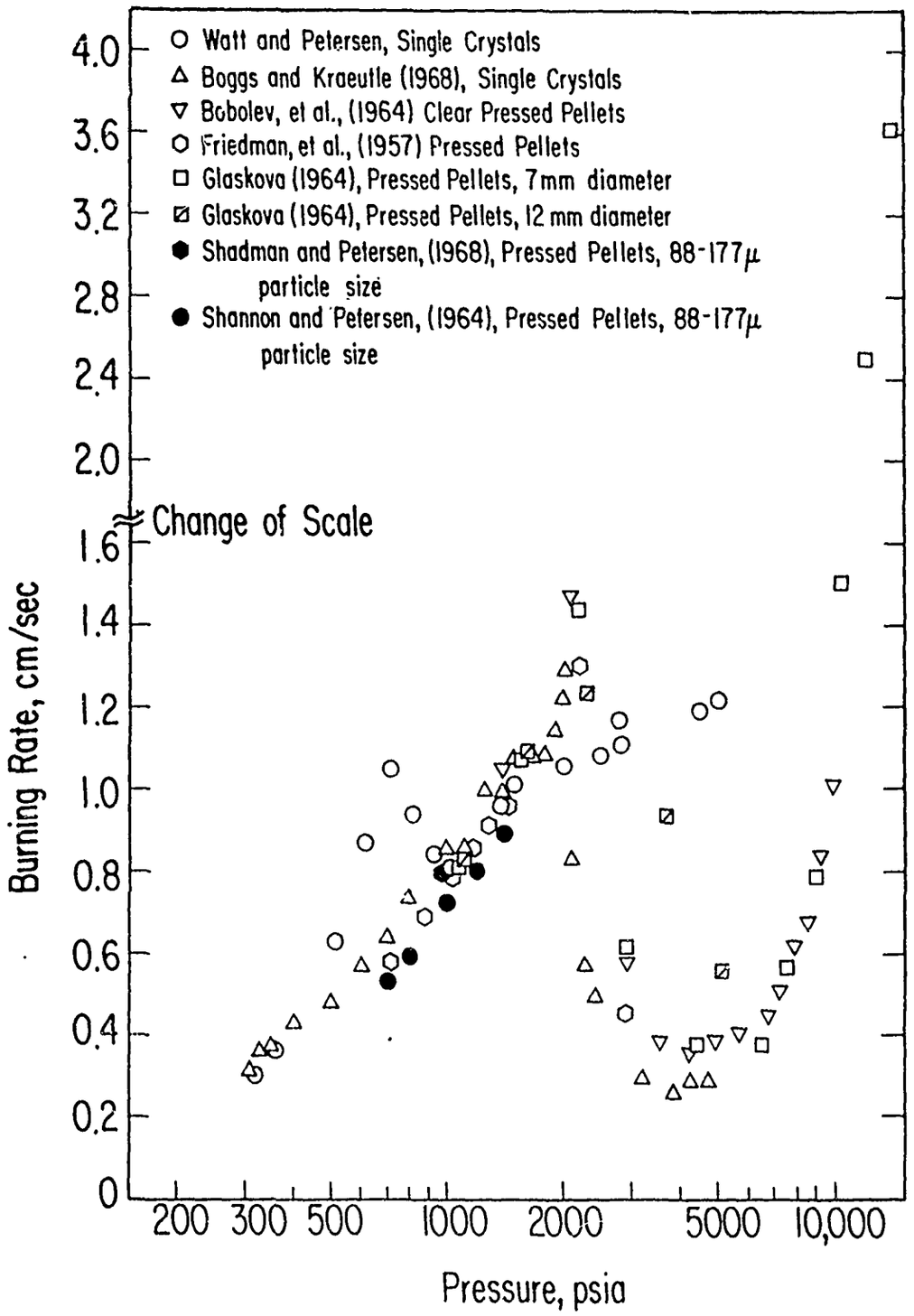

Fig. III-11. Comparison of room temperature burning rates of AP single crystals and pressed pellets.

Hightower and Boggs presented in reference (7) and the pressed pellet data indicates that, although interparticle effects may affect the exact deflagration velocity, they do not appear to have altered the fundamental shape of the burning rate isotherm. For both the single crystals and for the pressed pellets there appear to be two distinct deflagration mechanisms in which the burning rate increases with pressure and a transition region between these two mechanisms in which the burning rate decreases with increasing pressure.

Shannon and Petersen (45) made an extensive study of the effect of particle size on the burning rate of pressed pellets of AP. Their data reproducibly indicated that the burning rate increased with decreasing particle size, and their theory showed that extrapolation to zero particle size should give the burning rate of a single crystal. Extrapolation of their data using their theory to find the single crystal burning rate agreed quite well with the single crystal data of Hightower and Price (23). As an example of the experimental results of Shannon and Petersen (45), at 1000 psia the burning rate increased from 0.62 cm/sec with pellets pressed from 177-354μ AP powder to 0.84 cm/sec with pellets of 20-40 particles and extrapolated to 0.85 cm/sec for the single crystal. In burning single crystals of AP Hightower and Price (23) have presented considerable evidence for a molten zone of AP at the burning interface; if there is a similar molten zone at the burning surface of a pressed pellet, it is difficult to imagine how the size of the

particles in the bulk of the pellet could affect the burning rate of the molten AP at the surface. Hence, at present it is not clear why pressed pellets should burn at a different rate than single crystals, and possibly a comparison of the surface of quenched pellets with quenched single crystals as Hightower and Price (23) have done could help to clarify the difference.

Clearly Fig. III-11 indicates that there are larger differences between the different sets of data than could safely be accounted for simply by interparticle effects. In an effort to remove the influence of catalytic impurities Shadman and Petersen (43) recrystallized AP from three different suppliers and measured the burning rate of pellets pressed from the 88-177μ sieve fraction. After three recrystallizations the burning rate did not change with further recrystallization and the burning rate, 0.8 cm/sec at 1000 psia, was the same for all sources of AP. This value measured by Shadman and Petersen (43) for the burning rate at 1000 psia was distinctly different than the value measured by Shannon and Peterson (45) for the same particle size fraction; this comparison suggests the extreme difficulty in obtaining sufficiently pure AP to be certain of an intrinsic burning rate.

It appears that the catalytic influence of impurities in extremely low concentrations is the most logical explanation for the large differences between the data from this work and the remaining data shown in Fig. III-11. In

addition to the different location of the peak in the burning rate isotherm, the data from this work appear to be leveling off at high pressure rather than increasing nearly exponentially as indicated by the data of Bobolev (6) and Glaskova (17). The leveling off of the burning rate of the single crystals from the present work is supported by the low temperature data in Fig. III-5a in which the burning rate is essentially constant between 2000 and 5000 psia, the limit of the apparatus. Since it is apparent that there were important differences in impurity concentration or type of impurity between the AP single crystals grown at NWC and those grown in this program at UC, it is possible that successive partial recrystallizations may not be able to remove all catalytically active impurities. A study to test this possibility could involve the measurement of the burning rate of AP from various commercial suppliers as a function of successive partial recrystallizations. The burning rate of the AP from each source would be expected to approach a constant value after successive purification steps. If this constant burning rate was the same for all sources of AP, this would suggest that an intrinsic AP burning rate can be measured; but, if after successive partial recrystallizations the burning rate of the AP from the various sources did not approach the same value, this would indicate that successive recrystallizations cannot remove all the catalytically important impurities.

Conclusions

The AP single crystal burning rate isotherms showed striking parallelism as the pressure was increased, and the entire shape of the isotherms appeared to be compressed into a narrower range of pressures as the ambient temperature was lowered. The -28°C burning rate isotherm was horizontal above about 2000 psia and this suggested that the burning rate, rather than increasing without bound as pressure is increased, approached an asymptotic limit as the pressure was raised. A leveling off of the burning rate at 23 and 89°C (Fig. III-5a) was indicated near 5000 psia, but the apparatus could not be operated above this pressure to verify the possibility of a high pressure asymptotic limit for the AP burning rate.

The predominant peak in the burning rate isotherms separated two regions in which the burning rate increased with pressure, and at present there is no explanation for this apparent change in deflagration mechanism. In the lower pressure range the deflagration pressure limit seemed to occur at nearly a constant burning rate of about 0.2 cm/sec (Fig. III-8). The discontinuity in the -28°C isotherm suggested the possibility of a distinctly different pressure limit for deflagration at pressures above the pressure corresponding to the peak in the burning rate isotherm; this pressure limit appeared to occur at burning rates considerably above 0.3 cm/sec.

The AP single crystal burning rates were not affected

by pressurization with helium instead of nitrogen. The data were also identical when the burning interface receded horizontally instead of downwards. In addition, when AP single crystals grown at the University of California, Berkeley, were burned at the Naval Weapons Center there was very little change in the resulting burning rate data (Fig. III-10). Similar agreement resulted when crystals grown at the Naval Weapons Center were burned both at UC and at NWC. These results indicated that the measured burning rates were characteristic of the AP and were not influenced by conduction to the inert environment, natural convection, or the type of apparatus.

At room temperature the transition from the low pressure region of deflagration to the high pressure region occurred at about 2000 psia with the NWC crystals as compared to about 700 psia with the UC crystals. The data reported in the literature for AP pressed pellets tended to follow the shape of the burning rate isotherm for the NWC single crystals and the burning rate appeared to rise very rapidly above 5000 psia. In all cases extensive efforts were made to use pure AP; consequently it appeared that an important catalytic impurity was difficult to remove by recrystallization. Since it was shown that the differences in the data were not caused by the apparatus, both the data for the NWC crystals and for the UC crystals are significant and should form a basis for identifying catalytic impurities and for studying catalyzed AP deflagration.

CHAPTER IV

A PRELIMINARY STUDY OF THE CATALYTIC EFFECTS OF $KMnO_4$ ON THE DEFLAGRATION OF AMMONIUM PERCHLORATE

Introduction

The effect of catalysts on both the burning rate and the deflagration pressure limit of ammonium perchlorate has been the subject of a considerable amount of research. [See the review by Pittman (35).] Various additives give widely differing effects and the effect may be drastically altered by changing the concentration of the catalyst. Since the process of AP deflagration is not completely understood there is no satisfactory explanation for the effects of catalysts on the possible chemical reactions involved in AP deflagration. Of particular interest is the heterogeneous or homogeneous nature of the catalyzed reaction since a vast majority of this research has used pellets pressed from a mechanical mixture of AP and catalyst. Although there is growing evidence for a molten zone of AP at the burning surface (7), it might still be expected that the surface area of catalyst present, rather than the total mass, controlled the reaction rate. In these preliminary experiments the catalyst, potassium permanganate, was dispersed in the AP uniformly at the atomic level and also mechanically mixed with the AP to observe the effects of catalyst dispersion on deflagration.

Since $KMnO_4$ has the same crystal structure as NH_4ClO_4 it can be isomorphously substituted into the AP crystal

lattice. Considerable attention has been given to the thermal decomposition of AP single crystals doped with $KMnO_4$ (48) and of AP co-crystallized with $KMnO_4$ (41,47,51). These studies indicated that the rate of thermal decomposition increased as the fraction of $KMnO_4$ was increased from 0.5 mole % to 2 mole % (41,51). In addition, the activation energy for this process with 2 mole % $KMnO_4$ was found to be about 20 kcal/mole (41) at all temperatures studied; this value is extremely close to the value of 17-20 kcal/mole determined by Bircumshaw and Newman (4,5) for AP above 240°C in the cubic modification. Below this temperature Bircumshaw and Newman (5) found the activation energy for the thermal decomposition of orthorhombic AP to be 28-29 kcal/mole. In all cases the $KMnO_4$ considerably accelerated the thermal decomposition of the AP. At present it is not certain that the AP thermal decomposition is a step in the deflagration process; consequently a second objective of the present preliminary work was to compare the catalytic effects of $KMnO_4$ on AP deflagration with its reported effects on AP thermal decomposition.

Procedure

Large single crystals were grown with 0.4 mole % $KMnO_4$ isomorphously substituted in the AP lattice by a method very similar to that for growing pure AP crystals (Appendix A). A saturated aqueous solution of AP and $KMnO_4$ was used, and small AP crystals were used as the initial seeds. The

resulting purple crystals were quite opaque and consequently were difficult to test for flaws without cleaving them. The $KMnO_4$ also modified the rate of growth of the different crystal planes, thus changing the usual AP crystal habit; this made clean cleaving of the crystals considerably more difficult.

Imperfect crystals were powdered to make pellets with 0.4 mole % $KMnO_4$, and, for comparison, pellets were pressed with a mechanical mixture of 0.4 mole % $KMnO_4$ in AP. Pellets of 2 mole % $KMnO_4$ were also prepared from co-crystallized AP-$KMnO_4$ powder. In addition, a layered pellet was made by pressing pure AP powder on top of an AP-0.4 mole % $KMnO_4$ pellet; the pure AP section was ignited and this, in turn, ignited the AP-$KMnO_4$ section of the pellet.

The details of the combustion chamber and the photographic analysis are presented in Chapter III and Appendix A. The samples were ignited by a jet of hot nitrogen impinging normal to the pellet surface; details of the ignition apparatus and technique are presented in Appendix C.

Discussion of Results

The single crystals of AP with 0.4 mole % $KMnO_4$ isomorphously substituted into the crystal lattice, the pellets pressed from powder with 0.4 and 2 mole % $KMnO_4$ in AP, and the pellets pressed from a mechanical mixture of 0.4 mole % $KMnO_4$ in AP were ignited at either 1000 or 2000 psig and all failed to sustain deflagration. High-speed motion photography

indicated that with the hot gas impinging on the surface rapid decomposition would take place and occasional puffs of smoke would be emitted, but all reactions extinguished rapidly with the removal of the ignition gas jet.

In light of the catalytic effect of the $KMnO_4$ on the thermal decomposition of AP it seemed that while the hot ignition gas was striking the crystal or pellet surface the thermal decomposition provided a heat sink which prevented the surface temperature from reaching the ignition temperature. If deflagration is possible, a considerably stronger ignition stimulus may be necessary to overcome this heat sink effect. This consideration led to the experiments with the layered pellets in which the deflagrating AP section was used to ignite the catalyzed section of the pellet, and, again, the catalyzed pellet did not deflagrate. It is extremely difficult to prove that deflagration is not possible without definitive experimental results such as those discussed in Chapter II which delineated the low-pressure deflagration limit for pure AP and hence these results must be considered tentative. The possibility that a heat sink at the solid surface could prevent ignition is supported, at least qualitatively, by the ignition theory presented in Chapter V.

Similar results have been reported for AP catalyzed by NH_4MnO_4 (24). Consequently further studies to explore the basis for these results could be very fruitful. Possibly AP samples with extremely small percentages of $KMnO_4$ could be

made to deflagrate; then ignition delay, burning rate, and pressure limit data could be compared for pure AP and for AP with the per cent $KMnO_4$ increasing until ignition was impossible. Then, too, the effect of catalyst dispersion could be effectively studied as was originally planned for the present work. The results of such a study together with the existing data on the catalyzed thermal decomposition could lead to an increased understanding not only of the catalysis of AP deflagration but also of the mechanism of ignition and deflagration.

REFERENCES

1. Abramowitz, M., and Stegun, I. A., "Handbook of Mathematical Functions," National Bureau of Standards, Applied Mathematics Series 55 (1964).

2. Andersen, R., R. S. Brown, L. J. Shannon, "Ignition Theory of Solid Propellants," AIAA Solid Propellant Rocket Conference, January 1964, Preprint #64-156.

3. Beckstead, M. W., and J. D. Hightower, "Surface Temperature of Deflagrating Ammonium Perchlorate Crystals," AIAA J. 5, #10, 1785 (1967).

4. Bircumshaw, L. L., and Newman, B. H., "The Thermal Decomposition of Ammonium Perchlorate. I. Introduction, experimental, analysis of gaseous products, and thermal decomposition experiments," Proc. Roy. Soc. 227A, 115 (1954).

5. ————, "II. The kinetics of the decomposition, the effect of particle size, and discussion of results," ibid., A228 (1955).

6. Bobolev, V. K., A. P. Glaskova, A. A. Zenin, and O. I. Leypunsky, "A Study of the Temperature Distribution in the Combustion of Ammonium Perchlorate," Zh. Prikl. Mekhan. I Tekhn. Fiz., No. 3, 153 (1964).

7. Boggs, T. L., and K. J. Kraeutle, "Decomposition and Deflagration of Ammonium Perchlorate," NWC TP 4630 (1968), Naval Weapons Center, China Lake, Cal.

8. Boggs, T. L., personal communication, 1968.

9. Carslaw, H. S., and J. C. Jaeger, Conduction of Heat in Solids, Oxford University Press, London, 1959.

10. Engleman, V. S., "An Experimental and Theoretical Investigation of the Steady-State Deflagration of Single Crystals of Ammonium Perchlorate," Ph.D. Thesis, University of California, Berkeley, 1967.

11. Friedly, John C., "A Theoretical Analysis of Intermediate Frequency Instabilities During the Combustion of a Solid Propellant," Ph.D. Thesis, University of California, Berkeley, 1965.

12. Friedman, R., G. von Elbe, M. Hertzberg, and E. T. McHale, "Compcsite Solid Propellant Flame Microstructure Determination," Atlantic Research Corp., 1968 Annual Report for Contract NAS1-7457.

13. Friedman, R., "Mechanism of Solid Propellant Combustion" in Applied Mechanics Surveys, Spartan Books, Washington, D. C., 1966, pp. 1171-76.

14. Friedman, R., and J. B. Levy, "Research on Solid Propellant Combustion," AFOSR 2005, Contract AF49(638)-813 (Atlantic Research Corp.), 1961.

15. Friedman, R., R. G. Nugent, K. E. Rumbel, and A. C. Scurlock, "Deflagration of Ammonium Perchlorate," Sixth Combustion Symposium, Reinhold, 1956, p. 612.

16. Friedman, Raymond, "Experimental Techniques for Solid-Propellant Combustion Research," AIAA J. 5, 1217 (1967).

17. Glaskova, A. P., "Effect of Pressure on the Combustion Rate of Ammonium Perchlorate," Zh. Prikl. Mekhan. I Technich Fiz, No. 5, 153 (1963).

18. Gopalakrishnan, A., "Theoretical Studies on Solid Propellant Ignition," Final Report (NASA) Contract NAS-7-571 (1968), Consolidated Engineering Technology Corp., Mountain View, Cal., CETEC 2005-FR.

19. Hackman, E. E., and H. C. Beachell, "Combustion Characteristics of Crystalline Oxidizers," AIAA J. 6, #3, 561 (1968).

20. Hart, R. W., and F. T. McClure, "Combustion Instability: acoustic interaction with a burning propellant surface," J. Chem. Phys. 30, 1501 (1959).

21. Hermance, C. E., R. Shinnar, and M. Summerfield, "Ignition of an Evaporating Fuel in a Hot, Stagnant Gas Containing an Oxidizer," AIAA Solid Propellant Rocket Conference, January 1964, Preprint 64-118.

22. Hicks, Bruce L., "Theory of Ignition Considered as a Thermal Reaction," J. Chem. Phys. 22, 414 (1954).

23. Hightower, J. C., and E. W. Price, "Combustion of AP," Eleventh Symp. (Int.) on Combustion, Combustion Institute, Pittsburgh, Pa., 1967, p. 463.

24. Hightower, J. D., personal communication, 1968.

25. Horton, M. D., and E. W. Price, "Deflagration of Pressed Ammonium Perchlorate," Am. Rocket Soc. J. 32, 1745 (1962).

26. Huang, G. C., "Investigations of Heat-Transfer Coefficients for Air Flow Through Round Jets Impinging Normal to a Heat Transfer Surface," J. Heat Trans. 85C, 238 (1963).

27. JANAF Thermochemical Tables, The Dow Chemical Co., Midland, Mich.

28. Johnson, W. E., and Nachbar, W., "Deflagration Limits in the Steady Linear Burning of a Monopropellant with Application to Ammonium Perchlorate," Eighth Symposium on Combustion, p. 678, Williams & Wilkins (1960).

29. Johnson, W. E., and W. Nachbar, "Laminar Flame Theory and the Steady, Linear Burning of a Monopropellant," Arch. Rat. Mech. Anal. 12, 58 (1963).

30. Keenan, A. G., and R. F. Siegmund, "The Thermal Decomposition of Ammonium Perchlorate: A Literature Review," Dept. of Chem., Miami University, Coral Gables, SR 6, NONR 400807 (1968).

31. Lapidus, Leon, Digital Computation for Chemical Engineers, McGraw-Hill Book Co., Inc., New York, 1962.

32. Levy, J. B., and R. Friedman, "Further Studies of Pure Ammonium Perchlorate Deflagration," Eighth Symposium on Combustion, p. 663, Williams & Wilkins (1960).

33. Mayer, E., "A Theory of Flame Propagation Limits Due to Heat Loss," Combustion & Flame 1, #4, 438 (1957).

34. Micheli, P. L., "A Stop-Start Study of Solid Propellants," Aerojet-General Report NASA-CR-66487 (1967).

35. Pittman, Charles V., Jr., "The Mechanism of Decomposition of Ammonium Perchlorate: A Review," Propulsion Laboratory, Research and Development Directorate, U.S. Army Missile Command, Redstone Arsenal, Alabama 35809, Report No. RK-TR-66-13.

36. Powling, J., and W. A. W. Smith, "Measurement of the Burning Surface Temperatures of Propellant Compositions by Infrared Emission," Combustion and Flame 6, 173 (1962).

37. ———, "The Surface Temperature of Ammonium Perchlorate Burning at Elevated Pressures," Tenth Symp. (Int.) on Combustion, pp. 1373-1380, The Combustion Institute (1965).

38. Price, E. W., H. H. Bradley Jr., G. L. Dehority, and M. M. Ibiricu, "Theory of Ignition of Solid Propellants," AIAA Journal 4, #7, 1153 (1966).

39. Price, E. W., J. D. Hightower, K. J. Kraeutle, J. E. Crump, M. W. Beckstead, H. B. Mathes, and F. G. Buffum, "Combustion of Solid Propellants and Low Frequency

Combustion Instability," NOTS TP 4244 (1967), Naval Weapons Center, China Lake, Cal.

40. Rosser, Willis A., Jr., S. H. Inami, and H. Wise, "Thermal Diffusivity of Ammonium Perchlorate," AIAA J. 4, #4, 663 (1966).

41. Schmidt, W. G., and M. Stammler, "Thermal Decomposition of Catalyzed Ammonium Perchlorate," Bulletin of 21st Interagency Solid Propulsion Meeting, Vol. 1., pp. 71-88, June 1965 (CPIA Publication No. 71, May 1965).

42. Selzer, H., "The Temperature profile beneath the burning surface of an AP-composite propellant," 11th Symposium (Int.) on Combustion, Berkeley, Cal., August 14-20, 1966.

43. Shadman-Yazdi, F., and E. E. Petersen, personal communication, 1968.

44. Shannon, L. J., "Effects of Particle Size and Initial Temperature on the Deflagration of Ammonium Perchlorate Strands," Ph.D. Thesis, University of California, Berkeley, 1963.

45. Shannon, L. J., and E. E. Petersen, "Deflagration Characteristics of Ammonium Perchlorate Strands," AIAA J. 2, 168 (1964).

46. ————, "Burning Velocity of Ammonium Perchlorate Strands and Crystals," ibid., 6, 1594 (1968).

47. Shidlouskii, A. A., and L. F. Shmagin, Isv. Vysshikh Uchebn. Zavedenii, Khim. i Khim. Tekhnol., Vol. 5, No. 529, 1962 (CA 58, 5445e).

48. Smith, M. E., and E. E. Petersen, unpublished data, 1967.

49. Snedecor, G. W., Statistical Methods, The Iowa State Univ. Press, Ames, Iowa, 1956.

50. Spalding, D. B., "The Theory of Burning of Solid and Liquid Propellants," Combustion and Flame 4, 59 (1960).

51. Stammler, M., and W. Schmidt, "Oxidizer Properties that Affect Combustion Rates of Solid Propellants," presented at the Western States Combustion Meeting, April, 1966, Denver, Colo.

52. Summerfield, M., G. S. Sutherland, M. J. Webb, H. J. Taback, and K. P. Hall, "Burning Mechanism of Ammonium Perchlorate Propellants" in Solid Propellant Rocket Research (M. Summerfield, ed.), Academic Press, New York, 1960.

53. Torgesen, J. L., A. T. Horton, and C. P. Saylor, "Equipment for Single Crystal Growth from Aqueous Solution," J. Research of N.B.S. - c. Eng'g. and Instrumentation 67C, #1, 25 (1963).

54. Watt, D. M., Jr., "Ignition, Deflagration, and Deflagration Limits of Single Crystals of Ammonium Perchlorate," Ph.D. Thesis, University of California, Berkeley, 1969.

55. Whittaker, A. G., and D. C. Barham, "Burning Rate of Ammonium Perchlorate Single Crystals," ARS J. 32, #8, 1273 (1962).

56. Williams, F. G., Combustion Theory, Addison-Wesley, 1965.

57. Wooldridge, C. E., G. A. Marxman, and E. L. Capener, "Propellant Combustion Phenomena During Rapid Depressurization," Stanford Research Institute Report NASA-CR-66500 (1967).

APPENDIX A

Experimental Apparatus

A schematic diagram of the experimental apparatus (Fig. A-1) shows the high-pressure combustion chamber in which the AP was ignited by an electrically heated Chromel wire and the high-speed motion photographic system for measuring the AP burning rates. A detailed description of the apparatus follows.

The High-Pressure System

The combustion chamber was a 304 stainless steel cylinder 16" long with a 7" outside diameter and a 4" inside diameter. Both ends were threaded and fitted with stainless steel end plates, O rings, and threaded aluminum compression caps. The two windows were mounted in a cylinder perpendicular to the combustion chamber. The window housing was used to support the combustion chamber (Fig. III-1), and this permitted the combustion chamber to be rotated 360° to burn a sample in any desired orientation. The quartz windows (General Electric Co., Los Angeles) were sealed with Teflon packing (J. L. Doré Co., Houston, Texas) and gave a 3/4" aperture for photography. The entire combustion chamber was hydrostatically tested at 9600 psi to ensure safe operation up to 5000 psi.

An auxiliary stainless-steel surge tank, 24" long with a $5\frac{1}{2}$" outside diameter and a $4\frac{1}{2}$" inside diameter, was attached to the main combustion chamber to minimize pressure

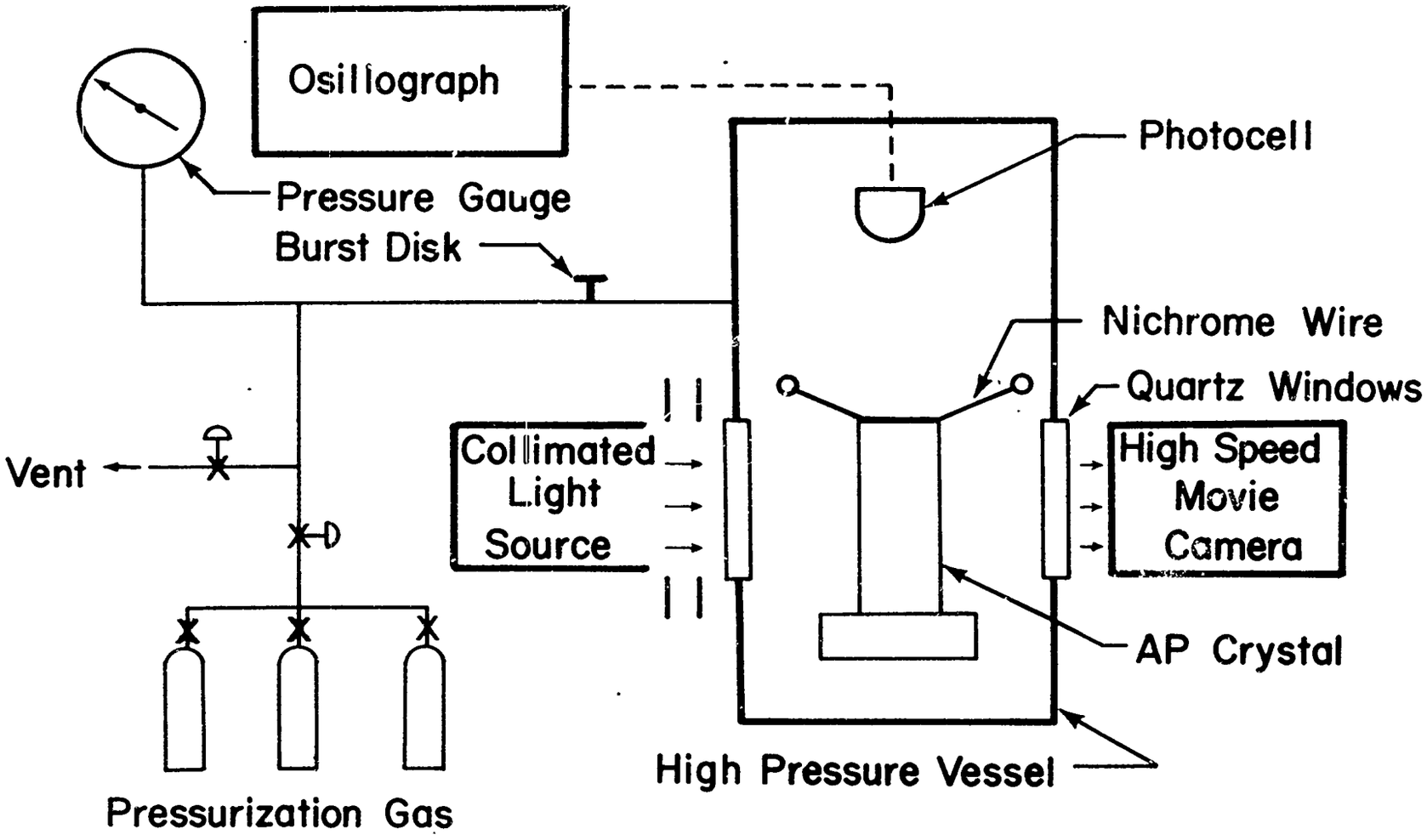

Fig. A-1. Schematic diagram of combustion apparatus for hot wire ignition.

fluctuations. This surge tank was hydrostatically tested at 6200 psi and was not used at pressures above 2500 psi.

All electrical connections were made through the end plates. The high-amperage electrode feedthroughs were Conax Exectrode Glands No. EG-093A-CU-T (Conax Corp., Buffalo, N.Y.), and the thermocouple and photocell feed through was a Conax Transducer Gland No. TG-20A8-T.

Aminco (American Instrument Co., Silver Spring, Md.) No. 44-1505 valves, fittings, and tubing, all with a working pressure rating of 60,000 psi, were used in the pressurization system. A 1/2" NPT burst disk assembly, BS and B Model WF-12 with muffled outlet (Black, Sivals, and Bryson, Kansas City, Mo.) was fitted on the combustion chamber to prevent overpressurization. The pressure was measured by a 5000-psig gauge with 0.1% of full-scale accuracy (Heise Bourdon Tube Co., Newtown, Conn.). Cylinders of nitrogen and helium were used for pressurization.

The combustion chamber was wrapped with electrical heating tape and with cooling coils through which refrigerant could be pumped. For the high- and low-temperature experiments the entire combustion chamber was insulated with glass wool, and for low-temperature experiments the windows were extended 4" beyond their housing with polished Lucite rod to prevent ice formation on the windows. A refrigeration unit with two-stage compression permitted operation at -50°C.

The Photographic System

A Hycam K2001R high-speed motion picture camera (Red Lake Laboratories, Santa Clara, Cal.), fitted with a footage indicator to facilitate multiple runs per roll of film, was used to photograph the AP burning. The camera was mounted on a Palmgren rotary table which was fastened to a rigid base; this permitted the camera to be rotated so that pictures could be taken of a title board labeling the pictures of each run with the experimental conditions (Fig. III-2). A 1" lens was used for photographing the title board and a 3" lens with 3/4" extension was used to photograph the burning. The light source was a slide projector modified to give collimated light. Timing light marks on the edge of the film every 1/120 second permitted accurate analysis of the AP burning rates.

A photocell was used to monitor the burning and to indicate when to turn the camera off. Either a photovoltaic cell, LS-223 (Texas Instruments Corp., Houston, Texas) or a photoresistor, CL-603A (Clairex Corp., New York, N.Y.) was used; a series of runs using both types of photocell simultaneously indicated that the slightly slower response of the photoresistor had no effect on the data. The photocell output was recorded on a Brush 842 two-channel oscillograph (Brush Instruments, Cleveland, Ohio) with 4410-66 plug-in preamplifiers. A preliminary estimate of the burning rate could be made by dividing the length of the AP crystal by the total burning time indicated by the photocell output.

Crystal Mounting and Ignition

The crystals were mounted on a steel block with a drop of Duco cement (Fig. III-3). An electrically heated Chromel wire was pressed against the crystal surface which was to be ignited.

Preparation of Single Crystals and Pressed Pellets

Large single crystals were grown from small AP seeds in a saturated water solution by lowering the temperature very slowly. This type of apparatus has been detailed completely in the literature (10, 39, 53). Perfect sections of these crystals were cleaved for burning by using a razor blade and a hammer. For burning purposes the crystals were typically 1.5 cm in length and 0.4 cm square in cross-section.

An Elmes Engineering 30-Ton Laboratory Hydraulic Press (Elmes Engineering, Detroit, Mich.) was used to dead-press the AP pellets to a density of 1.92 g/cc in a hardened-steel die with a 3/8" inside diameter.

APPENDIX B

Experimental Data

Table B-1 presents the data for Fig. III-5 in which the values are the averages of several runs.

Tables B-2, B-3, and B-4 present the actual experimental data used to compile Table B-1. Table B-5 presents the same data for the experiments using the crystals from the Naval Weapons Center in China Lake, California. The ambient temperature was measured by a thermocouple inside the combustion chamber. The variance tabulated in Tables B-2, B-3, B-4, and B-5 is the variance of a linear least squares fit to the photographic data for length of the crystal versus time during the deflagration. The burning rate is derived from this least squares fit of the photographic data. In addition, a second-order polynomial was fitted to the data and the variance of this fit was computed. If the burning rate was not constant throughout the length of the crystal, then the second-order polynomial should give a considerably better fit to the data, and its variance would be considerably smaller than that for the linear fit. The tabulated value of F is the ratio of the variance of the fit by the second-order polynomial to the variance of the fit by the first-order polynomial; since about 20 photographic data points were used in the least squares calculations, a value of F greater than about 3 indicates significant nonlinearity in the burning rate (49).

A value of F less than 3 indicates that the statement that the burning rate is constant is not contradicted by the data with 95% confidence.

The burning rate data, Tables B-2, B-3, B-4, and B-5, indicate an average variance of about 0.0001 cm^2 for the linear fit of the data. When the linear variance was this small, significant values of F (i.e., F greater than 3) were generally discounted somewhat since the accuracy of the data limited the ability to discern second-order effects. Those runs with large values of the variance and with values of F greater than 3 should definitely be considered suspect. Only those runs for which there was a clearly defined abnormality in the burning were discarded from these tables; this basically includes those runs where cracks developed in the crystal as a result of the thermal shock of ignition and significantly disrupted the burning process.

Those runs for which the hot wire ignition reproducibility did not cause the crystals to deflagrate completely have also been included in these tables. Although these data are not considered definitive, they appear to be significant because of their reproducibility.

Table B-6 presents the experimental data from which Fig. II-3 was drawn. T_H and T_C are the temperatures measured by the thermocouples at the hot and cold ends of the AP sample. Runs which reproducibly did not deflagrate significantly beyond the ignition wire are indicated by a footnote.

Table B-1. Summary of AP Single-Crystal Burning Rate Data

Pressure, psia	Temperature, °C	Burning Rate, cm/sec	Points
415	-28	0.33	2
465	-33	0.29	1
515	-29	0.38	2
565	-34	0.40	1
590 - 1500	-29	a	7
2030	-30	0.67[b]	3
2540	-30	0.66[b]	1
3040	-26	0.66[b]	2
3540	-30	0.67[b]	3
4040	-28.5	0.62[b]	2
4550	-26.5	0.64[b]	2
315	21	0.31	1
365	21	0.36	1
415	23	0.42	2
515	21.5	0.63	4
615	20.5	0.87	2
715	22.5	1.05	2
815	22.5	0.94	2
915	23	0.84	2
1015	23.5	0.806	5
1415	22.5	0.96	3
1515	24	1.01	1
2015	21.3	1.05	3

[a]Crystal did not deflagrate beyond ignition wire.

[b]At about 28°C between 2030 and 4550 psia the burning rate data changed so slightly that for graphical purposes these 13 data points have been averaged to give a constant burning rate of 0.65 cm/sec between 2030 and 4550 psia at -28°C.

Table B-1 concluded

Pressure, psia	Temperature, °C	Burning Rate, cm/sec	Points
2535	23.5	1.08	2
2785	23	1.17	1
2835	23	1.10	1
4535	22.5	1.19	3
5035	22.5	1.21	1
215	87	0.25	1
235	86	0.28	1
265	87	0.34	1
315	87	0.42	1
415	89	0.55	1
515	88	0.81	5
815	88.5	1.38	2
1015	90	1.44	6
1215	88	1.40	2
1415	92	1.24	3
2015	88	1.25	3
2535	86	1.30	2
3030	88	1.50	3
4030	87	1.53	2

Table B-2. AP Single-Crystal Burning Rate Data at Low Temperatures

(Vertical burning in nitrogen, hot wire ignition)

Pressure, psia	Temperature, °C	Burning Rate, cm/sec	σ^2 Variance x 10^4	F	Run No.
515	-16	0.45	2.1	1.0	610
1515	-10	a			531
2030	- 9.5	0.836	1.9	1.5	532
2030	-12	0.858	0.4	1.2	533
2030	- 9.5	0.846	0.2	1.0	534
3535	-11	0.77	3.2	1.6	536
3535	-12	0.77	1.0	2.6	537
420	-27	0.32	-	-	601
415	-28	0.335	3.5	3.6	612
465	-33	0.29	5.5	1.3	615
515	-28	0.38	-	-	602
515	-30	0.378	2.7	2.8	611
565	-34	0.40	0.2	1.0	614
590	-28	a			617
615	-29	a			613
1015	-47	a			511
1015	-29	a			584
1215	-50	a			512
1515	-26.5	a			530
1515	-32	a			585
2030	-35	0.64	0.7	1.6	541
2030	-28	0.68	0.01	1.4	542
2030	-26	0.69	0.75	1.1	543
2540	-30	0.66	0.6	4.0	590
3040	-26	0.67	0.6	1.4	589
3040	-26	0.65	0.5	1.0	592
3540	-37	0.65	0.4	1.6	538

[a]Crystal did not deflagrate beyond ignition wire.

Table B-2 concluded

Pressure, psia	Temperature, °C	Burning Rate, cm/sec	σ^2 Variance x 10^4	F	Run No.
3540	-25	0.697	0.8	5.3	539
3540	-29	0.65	1.1	4.9	540
4040	-28	0.64	1.1	1.6	591
4550	-25	0.65	1.5	1.6	586
4550	-28	0.63	0.6	6.5	587

Table B-3. AP Single-Crystal Burning Rate Data at Room Temperature

Press., psia	Temp., °C	Burning rate, cm/sec	Direction, horiz. or vertical	Gas, N_2 or He	σ^2 Variance x 10^4	F	Run No.
315	21	0.313	V	N_2	3.1	1.0	578
365	21	0.36	V	N_2	1.2	1.6	576
415	23	0.46	V	N_2	1.6	1.0	434
415	23	0.38	V	N_2	5.9	1.1	435
515	21	0.58	V	N_2	2.3	7.0	420
515	22	0.70	V	N_2	0.2	1.3	422
515	23	0.524	V	N_2	0.3	1.0	446
515	20	0.707	H	N_2	0.9	4.0	429
615	20.5	0.845	V	N_2	0.7	1.0	444
615	22	0.896	V	He	1.8	1.7	575
715	23	1.065	V	N_2	0.9	1.1	571
715	22	1.04	V	He	0.8	7.0	574
815	23	1.06	V	N_2	0.3	0.9	570
815	22	0.82	V	He	3.8	2.4	573
915	23	0.84	V	N_2	0.4	1.1	569
915	23	0.845	V	He	0.6	1.7	572

Table B-3 concluded

Press., psia	Temp., °C	Burning rate, cm/sec	Direction, horiz. or vertical	Gas, N_2 or He	σ^2 Variance x 10^4	F	Run No.
1015	23	0.748	V	N_2	0.6	1.3	406
1015	24	0.789	V	N_2	0.6	1.3	409
1015	22.6	0.798	H	N_2	0.4	1.2	417
1015	24	0.845	H	N_2	2.3	2.8	427
1015	25	0.85	V	He	2.8	2.6	551
1415	22	0.917	V	N_2	0.6	1.5	416
1415	21	0.988	H	N_2	2.5	5.8	430
1415	25	0.96	V	He	0.8	1.4	550
1515	24	1.01	V	He	1.6	1.6	549
2015	23.5	1.043	V	N_2	1.2	2.7	414
2015	19	1.017	V	N_2	0.8	1.0	419
2015	21.5	1.08	H	N_2	1.5	1.2	428
2535	23	1.073	V	N_2	0.4	1.0	413
2535	24	1.091	V	N_2	0.1	1.0	426
2785	23	1.17	V	N_2	1.1	3.4	425
2835	23	1.098	V	N_2	1.1	1.6	424
3030	23	1.01	V	N_2	5.6	3.5	410
4535	22	1.17	V	N_2	1.0	1.1	435
4535	22	1.22	V	N_2	0.6	1.8	436
4485	23	1.19	V	N_2	1.9	1.1	437
5035	22.5	1.21	V	N_2	1.9	1.8	431

Table B-4. Burning Rate Data at 90°C

(Vertical burning in nitrogen, hot wire ignition)

Pressure, psia	Temperature, °C	Burning Rate, cm/sec	σ^2 Variance x 10^4	F	Run No.
215	87	0.25	1.4	2	583
235	86	0.28	0.3	3	582
265	87	0.342	0.3	2.8	581
315	87	0.418	0.6	5.5	580
415	89	0.549	0.3	3.6	579
515	94	0.924	1.8	4.7	494
515	84	0.864	0.73	3.6	503
515	84	0.58	0.51	3.0	510
515	89	0.77	0.4	3.0	547
515	89	0.92	2.1	5.4	548
815	91	1.34	0.2	1.0	554
815	86	1.40	1 3	2.3	556
1015	90.5	1.54	3.4	2.9	495
1015	82	1.32	1.9	1.1	497
1015	100	1.43	2.7	1.9	502
1015	89.5	1.42	1.2	1.0	544
1015	90	1.45	0.6	1.4	545
1015	89	1.49	0.8	1.0	546
1215	88	1.40	3.3	1.5	553
1215	88	1.40	1.3	4.9	558
1415	86	1.23	1.6	1.1	496
1415	96	1.21	5.5	1.2	500
1415	93	1.28	1.0	1.0	552
2015	85.5	1.24	2.9	1.6	499
2015	90.5	1.27	11.1	1.1	501
2015	88	1.24	1.15	1.0	557

Table B-4 concluded

Pressure, psia	Temperature, °C	Burning Rate, cm/sec	σ^2 Variance x 10^4	F	Run No.
2535	84.5	1.22	4.1	1.1	498
2535	87	1.37	0.7	1.0	555
3030	91	1.49	0.5	1.3	506
3030	87	1.53	2.1	2.7	508
3030	85	1.47	.13	1.7	559
4030	87	1.49	2.0	1.0	504
4030	87	1.57	.74	2.1	505

Table B-5. AP Burning Rate Data - NWC Crystals
(Burned vertically in nitrogen, hot wire ignition)

Pressure, psia	Temperature, °C	Burning Rate, cm/sec	σ^2 Variance x 10^4	F	Run No.
515	22.5	0.522	1.1	1.0	421
1015	23.6	0.833	0.3	2.6	407
1015	23.6	0.832	0.1	1.4	408
2015	21	0.977	6.3	4.4	415
2015	20.8	0.957	7.2	1.0	423
2515	23.7	0.417	3.5	2.5	412
3000	23.0	0.338	1.3	1.0	411
5033	23.6	0.40	8.3	1.3	432
4945	22.5	0.37	9.0	2.7	433
4035	85	1.26	16.0	6.5	507

Table B-6. Deflagration Pressure-Limit Data

Pressure, psia	T_H, °C	T_C, °C	Length between thermocouples, cm	Length remaining, cm	Limiting solid temp., °C	Pellet or Crystal	N_2 or He	Run No.
193	91.0	52.5	2.19	1.54	79.6	P	N_2	469
200	81.5	64.5	1.83	0.86	72.5	P	He	480
200	80.0	33.2	2.20	1.71	69.6	P	N_2	468
216	72.0	18.5	2.25	1.56	55.5	P	N_2	466
226.5	64.0	32.0	2.26	1.12	48.0	C	N_2	477
238	56.7	16.0	2.20	1.32	40.4	P	He	465
245	42.4	20.5	1.64	1.10	35.3	P	N_2	457
246.5	47.0	24.0	2.29	1.31	37.2	C	N_2	478
250	42.0	20.2	2.26	1.46	34.2	P	N_2	458
255	48.5	23.0	1.93	0.94	35	C	N_2	600
273	38.5	1.5	2.23	1.20	21.5	P	N_2	459
283.5	37.5	4.5	1.89	0.63	16	C	N_2	599
299	32.5	2.5	2.14	0.30	6.8	P	N_2	462
302	32.5	1.3	2.33	0.41	6.8	P	He	464
310	15.5	-5.0	1.67	0.35	-0.7	C	N_2	472
311	30.2	-0.2	2.15	0.03	0.0	P	N_2	463
324	12.0	-13.0	2.14	0.34	-9.0	P	N_2	471
341	-1.5	-28.0	2.27	0.95	-16.8	P	N_2	476
386	-21	-50	2.39	0.74	-41	P	N_2	481

Table B-6 concluded

Pressure, psia	T_H, °C	T_C, °C	Length between thermocouples, cm	Length remaining, cm	Limiting solid temp., °C	Pellet or Crystal	N_2 or He	Run No.
815	-21	-36	1.74	1.62	a	C	N_2	603
830	-5.2	-31.5	1.58	0	-	C	N_2	604
1020	-9	-34	1.58	1.53	a	C	N_2	605
1020	1.0	-22	1.81	1.76	a	C	N_2	606
1020	3.0	-20	1.73	1.68	a	C	N_2	607

[a]Crystal did not deflagrate beyond ignition wire.

APPENDIX C

Comparative AP Burning Rates with Hot Gas Ignition

Introduction

The present research was a continuation of a project (10) using hot nitrogen to ignite the AP samples. With this technique the heat flux to the AP could be calculated using a measured heat transfer coefficient and could then be correlated with the measured ignition delay. The AP burning rate measured using this apparatus was distinctly different from the literature values (26) and from the results of the present work using hot wire ignition; consequently this technique was used only for comparative purposes. This section presents these results along with preliminary observations on the differences between the two ignition techniques.

Apparatus (10)

The only modification in the apparatus used for hot wire ignition was the addition of a metered nitrogen feed and an oven with a nozzle to direct the hot nitrogen at the AP sample (Fig. C-1). The output from the photocell at ignition triggered a relay in the control center (Fig. C-1) to turn off the solenoid valve controlling the flow of ignition gas; consequently the ignition gas did not affect the burning of the AP.

The oven (Fig. C-2), mounted inside the combustion chamber, was an Inconel tube, 4" long with an outside diameter of $1\frac{1}{2}$" and a wall thickness of 1/16". The Nichrome

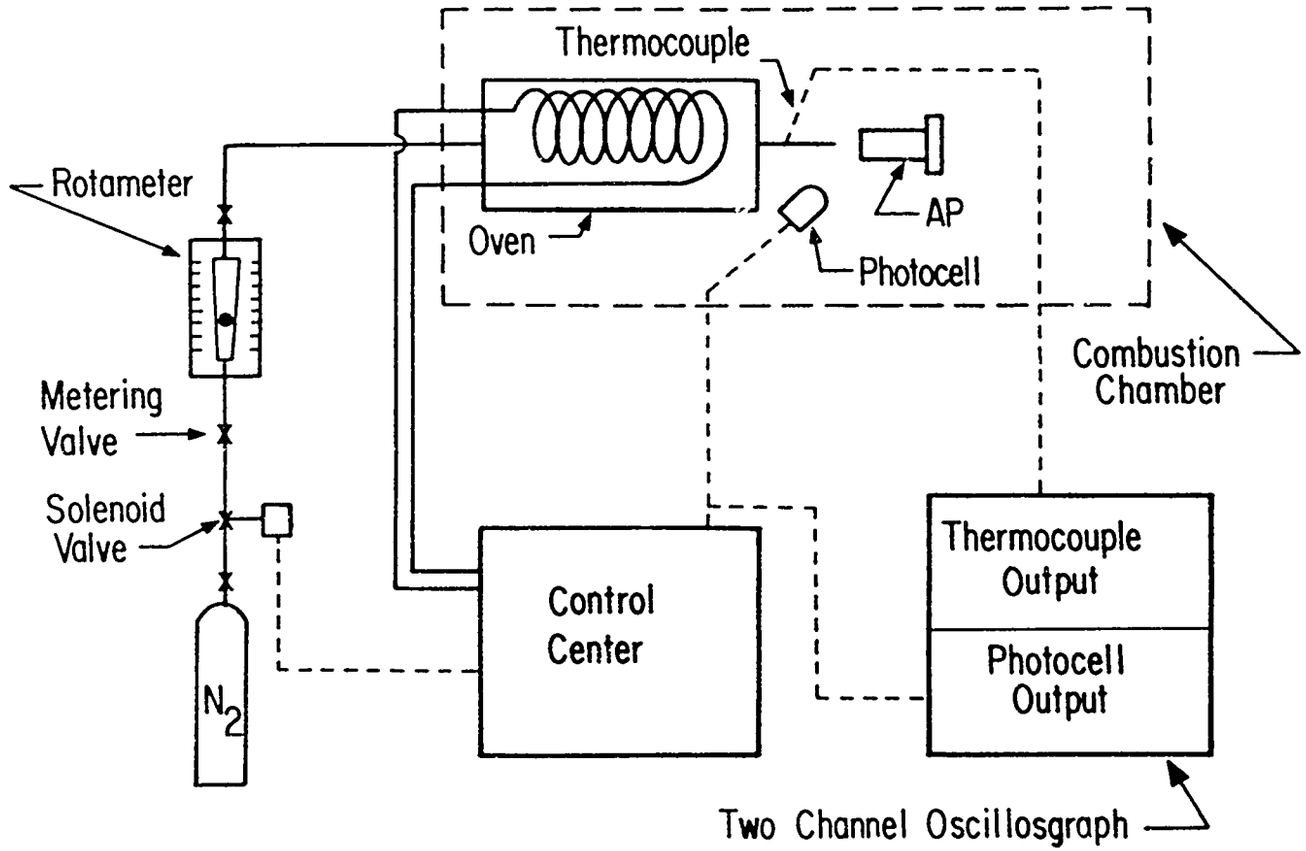

Fig. C-1. Schematic diagram of hot-gas ignition apparatus.

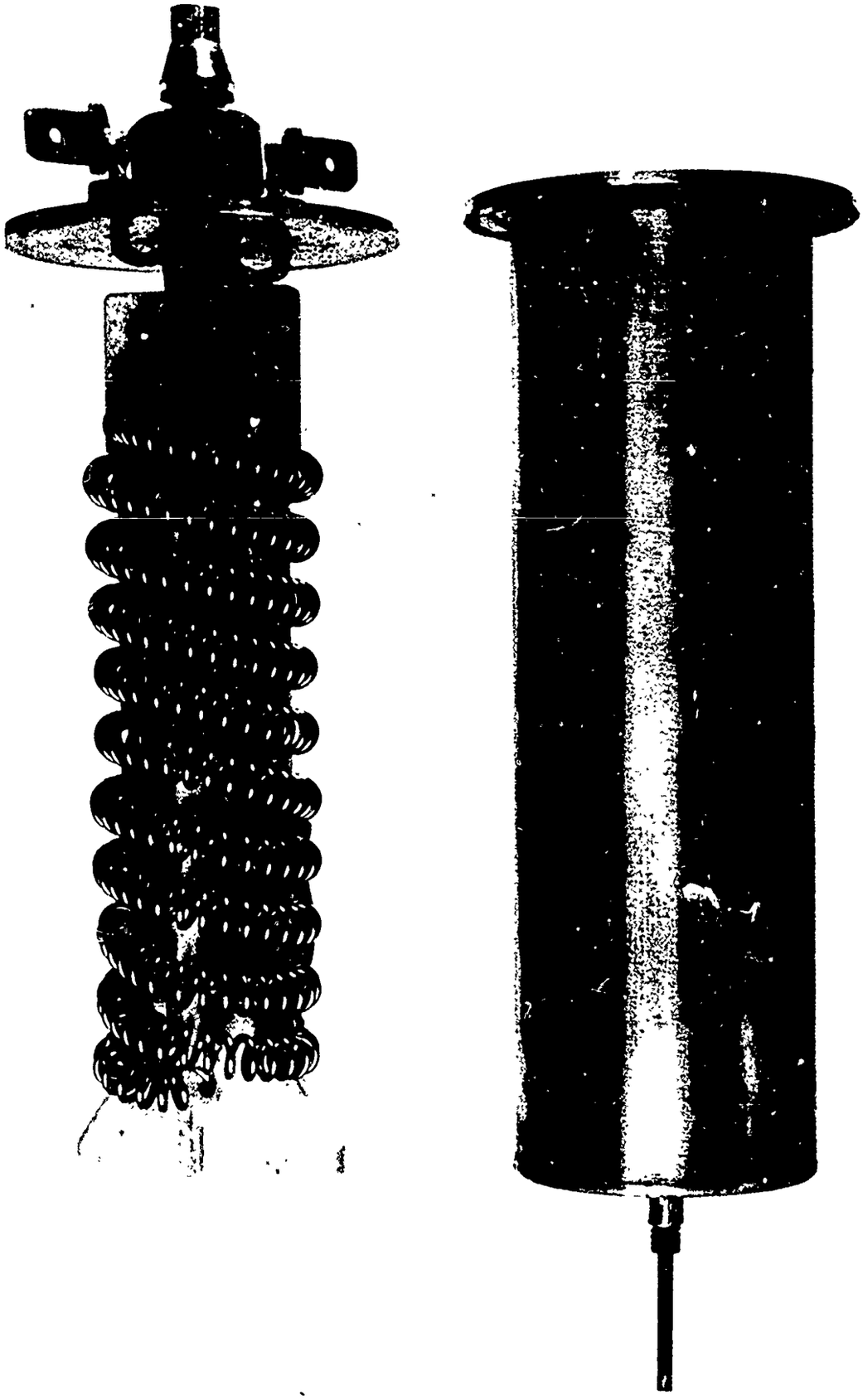

Figure C-2. Ignition gas heater.

heating coils were identical to those used in standard air heating "guns". The 1/16" nozzle was fitted with an Alumel-Chromel thermocouple to measure the temperature of the ignition gas.

A 500-psi pressure drop was maintained across the metering valve (Ideal Arrowsmith, Cheyenne, Wyo., Model PV-54-1-11) to assure a constant flow rate. A high-speed solenoid valve (Aktomatic Valve Co., Indianapolis, Ind., Model 1109, Type SBTDW) was used to turn the ignition gas on and off. A high pressure rotameter, Brooks Model 1452 (Brooks Instrument, Inc., Hatfield, Penn.) measured the flow of ignition gas. All components of the high pressure system had a safe working pressure rating of 5000 psi.

Procedure

The AP crystal was mounted 1/8" from the nozzle so that the gas would impinge normal to the surface (Figs. C-3 and C-4). The system was then pressurized and the gas flow was adjusted so that the Reynolds number in the nozzle remained constant at 5000 for all pressures.

With the gas flow off, the oven was preheated. The preheat time and the power input determined the temperature of the ignition gas which was confirmed by direct measurement. With the oscillograph on, the camera and ignition gas were turned on. The oven and ignition gas were turned off automatically by the photocell when ignition occurred.

The oscillographic and photographic data were analyzed in the same manner as with the hot wire experiments

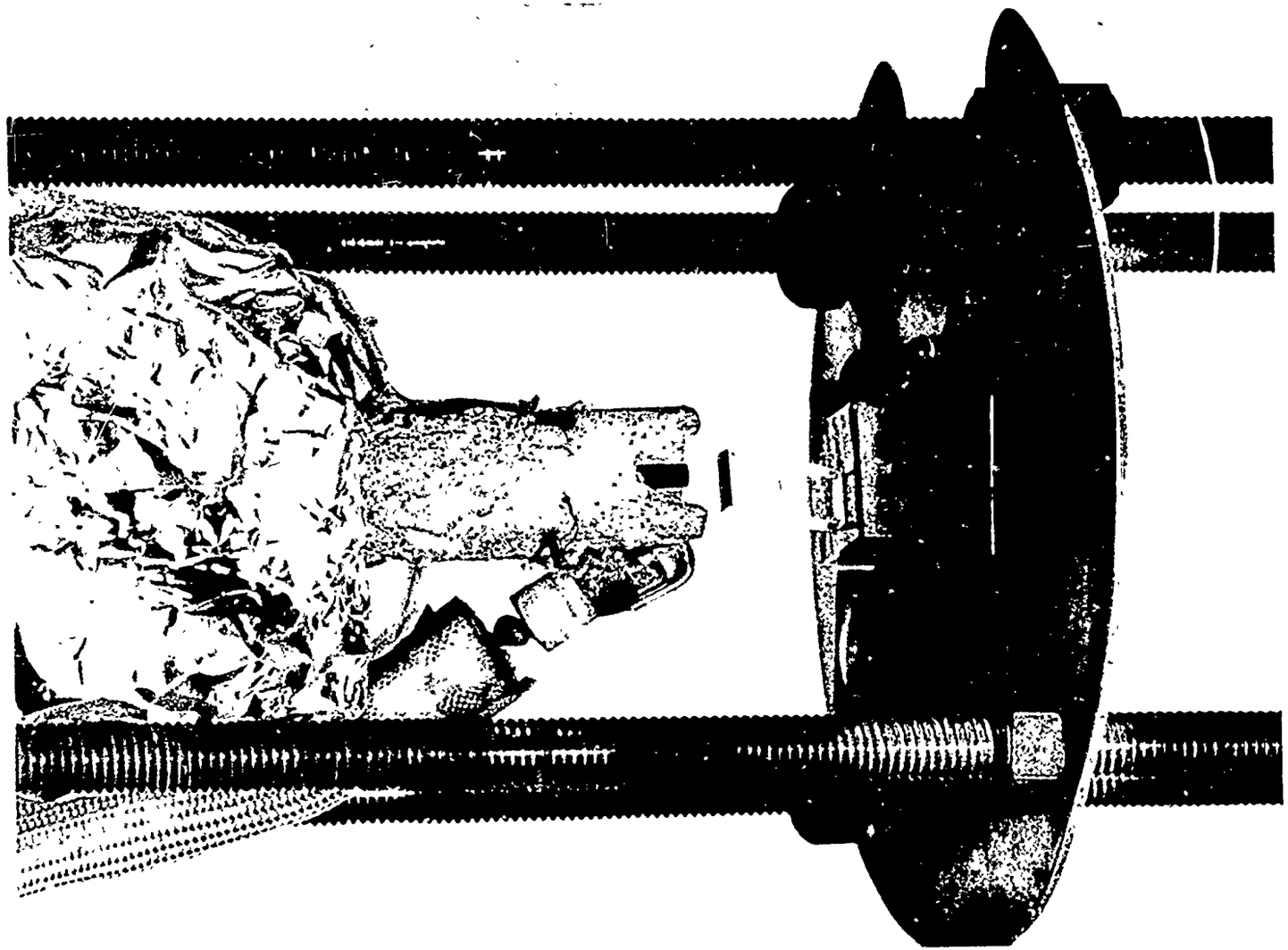

Figure C-3. Mounting of AP crystal for hot gas ignition.

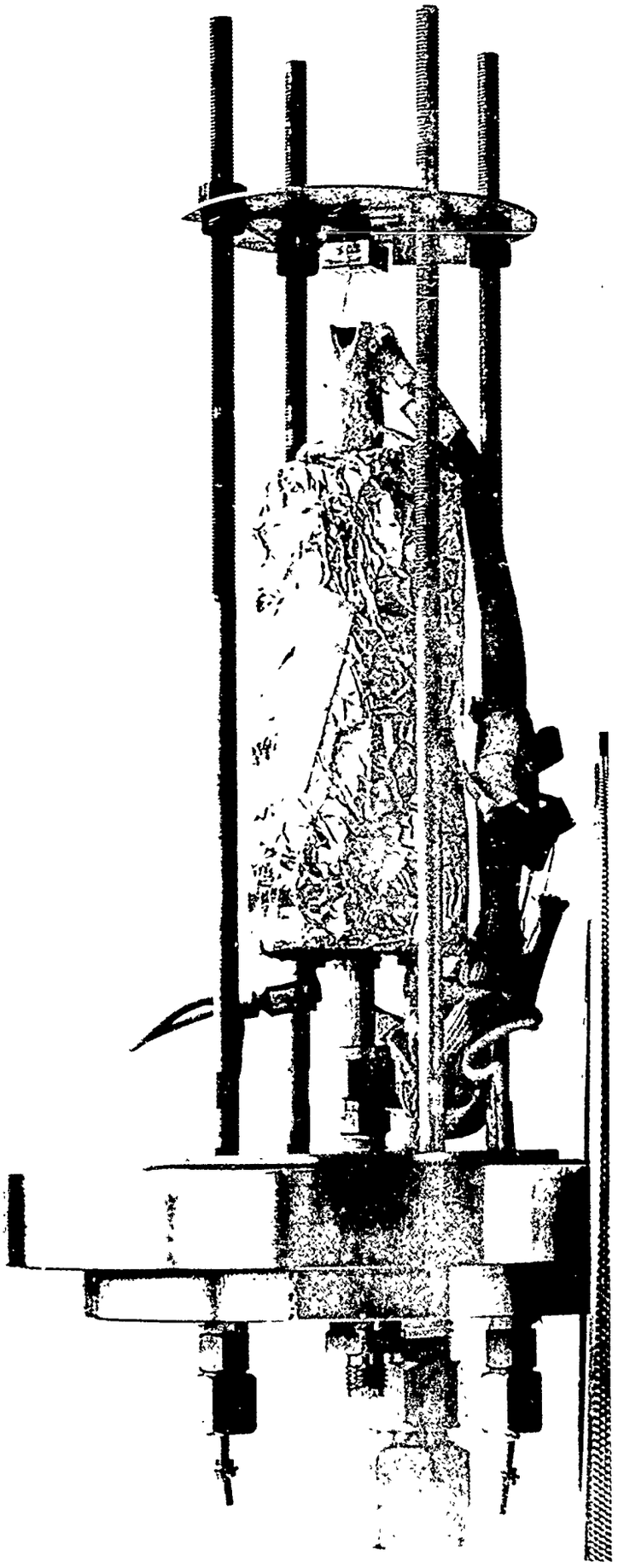

Figure C-4. Ignition heater assembly.

(see Chapter III). In addition, ignition delay data could be measured on the oscillogram as the time between turning on the ignition gas and the flash of light at ignition.

The previous work (10) did not have the high-speed motion picture camera and calculated all burning rates by dividing the length of the crystal by the duration of the deflagration indicated by the photocell output. Interpretation of the photocell output was somewhat arbitrary, and the acquisition of the camera has enabled the photocell data to be tested more fully.

Discussion of Results

The photographic analysis of the deflagration of three AP crystals at 1000 psig is shown in Table C-1. Although these results tend to substantiate Engleman's photocell data which averaged 1.15 cm/sec over 16 runs (10), only about 25% of the runs with hot gas ignition were photographically analyzable because excessive smoke obscured the AP sample throughout the burning. The unusually high variance in the photographic data may be attributed to the fact that, although the movies of the three runs in Table C-1 could be analyzed, the burning interface could be viewed only intermittently because of the smoke. As indicated by the data presented in Chapter III, continuous observation of the burning surface significantly improved the confidence in the measured burning rate.

Photography indicated that the oven used to heat the ignition gas altered the path of the flame's reaction

products and consequently set up convection currents of these hot reactive species. Apparently this turbulence caused the feedback of heat or reactive species to the flame zone and increased the deflagration rate. When all obstacles to the flow of reacted gas were removed and a hot wire was used for ignition, the burning surface could be viewed continuously throughout each run, but the burning rate decreased from 1.15 cm/sec to 0.8 cm/sec at room temperature and 1000 psig. Engleman's hot wire ignition data (10) agreed well with his hot gas ignition data because a steel plate holding the photocell was mounted at about the same distance from the AP sample as the oven when hot gas ignition was used. Evidently this created very similar hydrodynamic conditions and gave essentially identical burning rates.

In the present effort to understand the difference between the AP single crystal burning rate reported by NWC (23) and by Engleman (10) the plate holding the photocell was gradually moved further from the AP sample; as this was done, the smoke slowly ceased to recirculate back around the crystal and the burning rates gradually decreased. With the complete removal of obstructions to flow the burning rates were strictly comparable with those taken at the Naval Weapons Center as shown in Chapter III.

Before it was discovered that the apparatus was influencing the deflagration, significant burning rate data at an ambient temperature of 0°C was taken and the results

are tabulated in Table C-2. Under these conditions where the burning rate was considerably slower than at room temperature, the problem of smoke obscuring the burning interface was reduced, but not removed. Most runs could be analyzed photographically, but smoke intermittently obscured the entire burning process. The resulting burning rates at 0°C appear to follow the trend of the data presented in Chapter III, but it could not be determined if the apparatus influenced the deflagration process. Hence these data must be considered suspect until they are supported by independent measurements. It should be noted also that at 0°C the burning rates from the photocell data were usually higher than from the photographic data and could not be relied upon for accurate measurements.

This comparison of deflagration with an obstruction in the path of the reacting gases to deflagration with no obstructions to flow has strongly indicated that the turbulence generated by the obstruction can influence the deflagration processes. The effect appears to be less when the burning is slower either at lower pressures or lower temperatures. The interesting reproducibility of this effect may stimulate further research to understand why it occurs.

Table C-1. AP Single Crystal Burning Rate Data Using Hot Gas Ignition

(Horizontal burning, 23°C)

Pressure, psia	Photocell Burning Rate, cm/sec	Photographic Burning Rate, cm/sec	Variance (Photos) $\sigma^2 \times 10^4$	Run No.
1015	1.0	1.20	4.0	393
1015	1.1	1.12	8.4	401
1015	1.17	1.13	6.1	403
1015	1.15	-	-	a

[a]Ref.

Table C-2. AP Single Crystal Burning Rate Data Using Hot Gas Ignition

(Horizontal burning, 0°C)

Pressure, psia	Photocell Burning Rate, cm/sec	Photographic Burning Rate, cm/sec	Variance (Photos) $\sigma^2 \times 10^4$	Run No.
515	0.61	a	-	237
515	0.66	0.65	0.4	245
515	0.64	0.56	0.45	247
515	-	0.63	12.0	252
515	0.62	0.59	3.2	255
715	-	0.70	9.0	240
715	1.1	0.98	0.2	241
715	0.91	0.76	3.0	243
1015	0.82	0.60	1.3	231
1015	0.80	0.66	3.9	232
1015	0.85	a	-	233
1015	0.78	0.59	16.	234
1015	0.84	0.61	1.0	235
1015	0.75	0.53	2.0	244

Table C-2 concluded

Pressure, psia	Photocell Burning Rate, cm/sec	Photographic Burning Rate, cm/sec	Variance (Photos) $\sigma^2 \times 10^4$	Run No.
1015	0.83	0.66	0.5	256
1015	0.89	0.69	2.3	258
2015	1.11	a	-	248
2015	1.14	a	-	249
2015	1.19	a	-	250
2015	2.3	a	-	251
2015	1.1	1.05	1.0	253
2015	1.56	1.51	5.0	254
2015	1.3	1.56	20.	257

[a]Smoke obscured the burning surface.

UNCLASSIFIED

Security Classification

DOCUMENT CONTROL DATA – R & D

Security classification of title, body of abstract and indexing annotation must be entered when the overall report is classified.

1. ORIGINATING ACTIVITY (Corporate author)	2a. REPORT SECURITY CLASSIFICATION
University of California Department of Chemical Engineering Berkeley, California 94720	UNCLASSIFIED 2b. GROUP

3. REPORT TITLE

DEFLAGRATION AND DEFLAGRATION LIMITS OF SINGLE CRYSTALS OF AMMONIUM PERCHLORATE

4. DESCRIPTIVE NOTES (Type of report and inclusive dates)
Scientific Final

5. AUTHOR(S) (First name, middle initial, last name)
David M Watt Jr
Eugene E Petersen

6. REPORT DATE	7a. TOTAL NO. OF PAGES	7b. NO. OF REFS
30 June 1968	100	57

8a. CONTRACT OR GRANT NO. AF-AFOSR-959-65	9a. ORIGINATOR'S REPORT NUMBER(S)
b. PROJECT NO. 9750-02	
c. 6144501F	9b. OTHER REPORT NO(S) (Any other numbers that may be assigned this report)
d. 681308	AFOSR 69-0756TR

10. DISTRIBUTION STATEMENT
1. This document has been approved for public release and sale; its distribution is unlimited.

11. SUPPLEMENTARY NOTES	12. SPONSORING MILITARY ACTIVITY
TECH, OTHER	AF Office of Scientific Research (SREP) 1400 Wilson Boulevard Arlington, Virginia 22209

13. ABSTRACT

Using a new technique, the deflagration pressure limit was measured by imposing a known linear temperature gradient along the length of the AP sample and igniting the warmer end. The pressure was adjusted so that the flame would not propagate through the entire solid, and the length remaining unburned determined the limiting solid temperature corresponding to the set pressure. For both AP single crystals and pressed pellets the limiting pressure fell essentially linearly from 35 psia to 10 psia over the solid temperature range of -40 to 50°C, and from 50 to 80°C the slope of the limiting pressure versus the solid temperature decreased considerably. No difference was observed when using helium in place of nitrogen as the ambient atmosphere.

The AP single crystal deflagration rates were measured using high-speed motion photography and were essentially the same in helium and nitrogen ambient atmospheres. As the pressure was increased the burning rate increased, went through a maximum and a minimum, and then continued to increase. The burning rates increased monotonically with increasing ambient temperature.

Comparison of AP single crystal burning rates with another laboratory indicates that catalytically active impurities were present in the single crystals even though the impurity concentration was extremely low.

In direct contrast to the catalytic effect of $KMnO_4$ on AP thermal decomposition, a preliminary study showed that 0.4-2.0 mole % $KMnO_4$ isomorphously substituted into the AP crystal lattice prevented deflagration from occurring.

DD FORM 1 NOV 65 1473

UNCLASSIFIED

Security Classification

UNCLASSIFIED

Security Classification

14. KEY WORDS	LINK A		LINK B		LINK C	
	ROLE	WT	ROLE	WT	ROLE	WT
Solid Propellant						
Single Crystals						
Ammonium Perchlorate						
Deflagration Rates						
Deflagration Limits						

Security Classification